

UNIVERSITÀ DEGLI STUDI DI GENOVA

SCUOLA POLITECNICA

DIME

**Dipartimento di Ingegneria Meccanica, Energetica,
Gestionale e dei Trasporti**



**MASTER OF SCIENCE THESIS
IN
MECHANICAL ENGINEERING**

**Reliability improvement of gas turbine performance
monitoring based on online measurement data
processing**

Supervisor:

Dr. Cyrille Jerome Bricaud – Ansaldo Energia Switzerland

Chiar.mo Prof. Ing. Alessandro Bottaro

Candidate:

Diego Fancello

March 2024

In collaboration with:

ansaldo | energia

Miglioramento dell'affidabilità del monitoraggio delle prestazioni delle turbine a gas basato sull'elaborazione dei dati di misura online

Sommario

Le turbine a gas rivestono un ruolo cruciale nella produzione dell'energia elettrica e sono un prodotto ingegneristico estremamente complesso che lavora in condizioni di stress termico e meccanico elevato. Queste condizioni ne causano inevitabilmente la degradazione nel tempo. Tale deterioramento influisce sulle prestazioni delle turbine e può portare alla rottura di componenti, con conseguente potenziale inattività dell'impianto e ingenti perdite economiche per il cliente e il produttore. È pertanto essenziale disporre di un sistema di monitoraggio in grado di valutare lo stato di salute di tali macchine e intervenire tempestivamente in caso di significativa diminuzione delle prestazioni. Per valutare le performance delle turbine, è necessario avere a disposizione un software di calcolo e acquisire misurazioni. Tuttavia, queste misurazioni sono spesso soggette ad errori dovuti alla normale degradazione del sensore o alla sua eventuale rottura. Questo lavoro di tesi si focalizza sull'elaborazione delle misurazioni per individuare eventuali problematiche e intervenire al fine di migliorare l'affidabilità dei risultati. Sono stati dunque definiti criteri per identificare le misurazioni errate e rielaborarle in modo appropriato. È stata dimostrata l'efficacia del sistema di preprocessamento ed è stato dunque svolto un confronto tra i risultati dei calcoli ottenuti da misure grezze e da misure elaborate, per valutarne gli effetti. Inoltre, nel lavoro di tesi è stata sviluppata anche una parte di automazione del processo di monitoraggio attraverso codice python, che permette di scaricare dal database le misure automaticamente ed elaborarle. È stata anche dimostrata l'efficacia del performance tool nell'identificare la degradazione, che ne sottolinea l'importanza dello sviluppo di un sistema di preelaborazione delle misurazioni per migliorarne l'affidabilità. Infine, vengono esplorati possibili sviluppi futuri per migliorare ulteriormente l'affidabilità e l'automazione del sistema di monitoraggio.

Reliability improvement of gas turbine performance monitoring based on online measurement data processing

Abstract

Gas turbines play a crucial role in power generation and are an extremely complex engineering product working under high thermal and mechanical stress conditions. These conditions inevitably cause them to deteriorate over time. Such deterioration affects turbine performance and can lead to component failure, potentially resulting in plant shutdown and huge economic losses for the customer and the manufacturer. It is therefore essential to have a monitoring system that can assess the health of these machines and intervene promptly in the event of a significant drop in performance. To assess the performance of turbines, it is necessary to have calculation software available and to acquire measurements. Nevertheless, these measurements are often subject to errors due to normal sensor degradation or failure. This thesis work focuses on the processing of measurements in order to identify possible problems and take action to improve the reliability of the results. Criteria were therefore defined to identify erroneous measurements and reprocess them appropriately. The effectiveness of the pre-processing system was demonstrated, and a comparison of the calculation results obtained from raw measurements and processed measurements was therefore carried out to evaluate the effects. In addition, an automation part of the monitoring process was also developed in the thesis work using python code, which allows measurements to be downloaded from the database automatically and processed. The effectiveness of the performance tool in identifying degradation was also demonstrated, which underlines the importance of developing a system to pre-process the measurements in order to improve their reliability. Finally, possible future developments are explored to further improve the reliability and automation of the monitoring system.

Acknowledgements

Termino con gioia grazie a questo elaborato un lungo e impegnativo percorso. Desidero esprimere il mio profondo ringraziamento a tutte le persone che mi hanno accompagnato, sostenuto e creduto in me. Innanzitutto, alla mia famiglia, da cui ho imparato la determinazione e il valore del duro lavoro, che mi hanno permesso di affrontare e superare le sfide di questo percorso con risultati soddisfacenti. Un pensiero speciale va a coloro che purtroppo non sono più con noi, ma che rimarranno sempre nel mio cuore. Un ringraziamento sentito va anche agli amici e colleghi universitari, che mi hanno sempre sostenuto e con cui ho condiviso un legame di stima e rispetto reciproco. Un grazie speciale va al Prof. Ing. Alessandro Bottaro, di cui ho la massima stima, per avermi concesso l'opportunità di svolgere la mia tesi presso Ansaldo Energia Switzerland nei mesi passati. La sua fiducia e il suo sostegno sono stati fondamentali per il mio percorso. Infine, desidero ringraziare di cuore il team di Ansaldo Energia Switzerland per avermi offerto questa preziosa opportunità e per avermi guidato durante il mio lavoro di tesi, che mi ha permesso di imparare e crescere professionalmente. Un ringraziamento particolare va a Stefan Rofka, Michael Lupori e Cyrille Bricaud, ingegneri eccezionali e persone straordinarie.

I gladly end a long and challenging journey with this thesis. I would like to express my deepest thanks to all the people who have accompanied me, supported me and believed in me. First of all, to my family, from whom I learnt determination and the value of hard work, which enabled me to face and overcome the challenges of this journey with satisfying results. A special thought goes to those who are unfortunately no longer with us, but who will always remain in my heart. Heartfelt thanks also go to my friends and university colleagues, who have always supported me and with whom I shared a bond of mutual esteem and respect. A special thanks goes to Prof. Ing. Alessandro Bottaro, whom I hold in the highest esteem, for giving me the opportunity to do my thesis at Ansaldo Energia Switzerland over the past few months. His trust and support have been fundamental for my path. Finally, I would like to sincerely thank the team at Ansaldo Energia Switzerland for offering me this valuable opportunity and for guiding me during my thesis work, which allowed me to learn and grow professionally. My special thanks go to Stefan Rofka, Michael Lupori and Cyrille Bricaud, exceptional engineers and extraordinary people.

Contents

Sommario	I
Abstract	II
Acknowledgements	III
1 – Introduction	1
1.1 – Ansaldo Energia Switzerland.....	1
1.2 – Gas Turbine introduction.....	2
1.2.1 – Thermodynamic cycle.....	3
1.2.2 – Gas Turbine plant.....	6
1.2.2.1 – The compressor.....	9
1.2.2.2 – The combustor.....	11
1.2.2.3 – The turbine.....	12
1.2.3 – Combined cycle plant	16
1.3 – Gas Turbine monitoring.....	18
1.3.1 – Motivation.....	18
1.3.2 – Gas Turbine issues.....	19
1.3.3 – Problem definition.....	21
2 – Performance monitoring tool	25
2.1 – Instrumentation.....	25
2.1.1 – Pressure measurements.....	25
2.1.2 – Temperature measurements.....	26
2.1.3 – Fuel measurements.....	27
2.1.4 – Mass flow measurements.....	27
2.1.5 – Other measurements.....	27
2.1.6 – General requirement measurements.....	28
2.2 – Gas Turbine model	29
2.2.1 – Heat balance.....	30
2.2.1.1 – Intake system.....	33
2.2.1.2 – Compressor.....	34

2.2.1.3 – Combustor.....	35
2.2.1.4 – Turbine.....	36
2.2.1.5 – Diffuser.....	38
2.2.1.6 – Secondary air system.....	39
2.2.1.7 – Exhaust system.....	39
2.2.2 – Synthesis.....	41
2.2.3 – Ansyn factor.....	42
2.3 – Solver.....	43
3 – Automated heat balance.....	45
3.1 – Description.....	45
3.2 – Results	54
4 -Conclusions.....	63
References....	64
Nomenclature.....	65

1. Introduction

1.1 – Ansaldo Energia Switzerland

The activity described in this thesis was developed in collaboration with Ansaldo Energia, Switzerland AG. The department emerged in 2016 from the acquisition of intellectual properties related to Alstom's heavy-duty advanced gas turbines owned by General Electric, specifically concerning the GT26 and GT36 turbines. Ansaldo Energia is a world leader in the production of power generation plants. Its field of expertise includes power plant design and construction, machinery and equipment manufacturing, and strategic services related to these activities. The main products designed and built by the company involve gas turbines, steam turbines, and electric generators. Ansaldo Energia offers a full range of heavy-duty gas turbines (GT) for power generation applications, from E-class to H-class technology, with power ratings from 80 MW to 538 MW in single-unit configuration. This enables customers to operate both open-cycle and combined-cycle plants equipped with the latest generation of gas turbines featuring high performance in terms of efficiency, power, emissions reduction, flexibility in fuel use, and economic efficiency.







Gas Turbine	Gas Turbine Performance	Power Plant Configuration	Power Plant Performance
GT36-S6 	369 MW 42.3%	1+1	520 MW 62.3%
		2+1	1,046 MW 62.6%
GT36-S5 	538 MW 42.8%	1+1	760 MW 62.6%
		2+1	1,525 MW 62.8%
GT26 	370 MW 41.0%	1+1	540 MW 61%
		2+1	1,083 MW 61.2%
AE94.3A 	340 MW 40.3%	1+1	495 MW 60%
		2+1	992 MW 60.3%
AE94.2 	190 MW 36.3%	1+1	287 MW 55.8%
		2+1	578 MW 56.2%
AE64.3A 	80 MW 36.4%	1+1	120 MW 55.7%
		2+1	243 MW 56.4%

Figure 1.1 – Ansaldo Energia Gas Turbine Sheet [1]

The GT26 turbine (Fig. 1.1) belongs to class F and features a single sequential combustor that allows it greater flexibility and extends the operating window in compliance with regulations. It features 22 stages of axial compressor with 4 variable guide vanes for greater regulation in part load, 1 stage of HPT and 4 stages of LPT. It has fuel flexibility that allows it to burn a mixture of natural gas with 45% hydrogen. The GT36 (Fig. 1.2) represents the evolution of the GT26, belongs to the H class and is the most powerful in Ansaldo Energia's portfolio. It features 15 axial compressor stages with 4 variable guide vane and 4 turbine stages, through its sequential canular combustor it manages to keep emissions low and increases its operational flexibility. It gets to burn up to 70 percent hydrogen in mixture with natural gas.

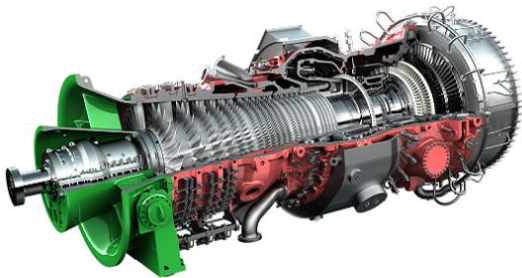


Fig. 1.2 – Ansaldo Energia GT26 [1]

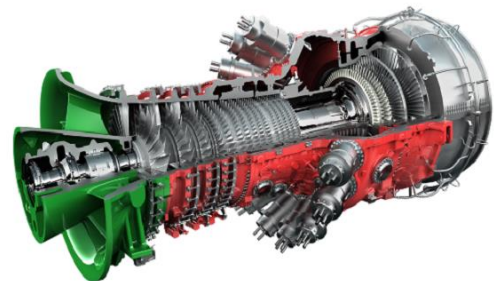


Fig. 1.3 – Ansaldo Energia GT36 [1]

Along with the product, Ansaldo Energia, provides customers with a remote monitoring and diagnostic service in order to detect early signs of failure, thus reducing downtime and safeguarding the customer with predictive maintenance. The following work focuses on the remote monitoring of GT36 performance employed at the Marghera and Presenzano plants. These thermoelectric power plants are among the most efficient in Europe and can generate 760 MW with an efficiency of about 62.6 percent.

1.2 – Gas Turbine introduction

A gas turbine is an internal combustion machine that transforms chemical energy from fuel by turbomachinery. This energy can be exploited in different ways depending on the application. In the case of aeronautical application, it is harnessed to generate thrust by expanding gases in a nozzle or converting it into mechanical energy to move a propeller. The other main application is for power generation, in fact the energy released is used to put the shaft into rotation, which in turn moves an electricity generator, which feeds electricity into the grid that we use every day. They are also very often used in industrial applications to move mechanical organs such as pumps or compressors and as propulsion systems for ships, tanks and trains.

Over the years gas turbines have found increasing use in power generation, aided by the fact that technological development has made it possible to achieve high performance, resulting in reduced exhaust emissions, an important feature given today's problems due to climate change. As such, there is an ongoing race for hydrogen by leading manufacturers of gas turbines to reduce emissions. Given their small size, they favor concentrated production, allowing power generation close to the point of consumption, reducing transmission losses. In fact, they turn out to be among the power generation systems with the best power-to-weight ratio. Another peculiarity is that they can adapt to fluctuations in grid demand. Finally, combined cycle applications have made it possible to achieve very high thermodynamic efficiencies, making GTs an important player in power generation.

1.2.1 The thermodynamic cycle

Underlying the operation of gas turbines is the ideal Brayton-Joule cycle, which consists of the following transformations of a gas: an adiabatic compression (1-2), heating at constant pressure (2-3), adiabatic expansion (3-4), and heat transfer at constant pressure (4-1). A Brayton cycle is shown in Figure 1.2.

Such a cycle is called ideal because, it exploits the concepts of ideal machine and ideal gas. Ideal machine means that there are no energy losses during internal processes; therefore, there are no heat losses during isobaric phases and the compression and expansion processes are isentropic. By ideal gas is meant that the gas complies with the perfect gas equation, has constant specific heat at constant pressure (c_p) and constant volume (c_v), which means that their ratio (γ) remains constant in the cycle, and finally does not undergo transformations of state or gas composition.

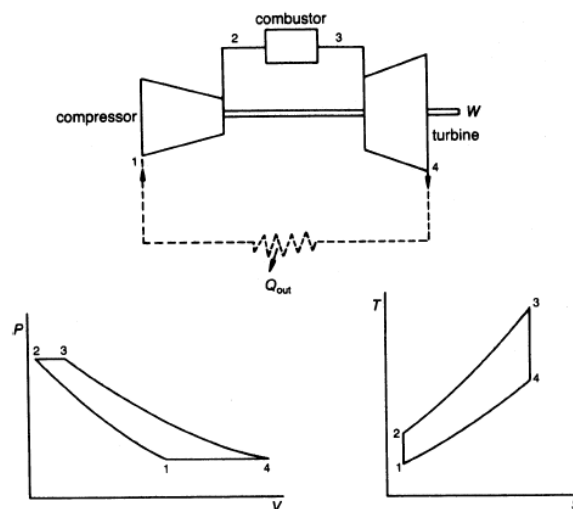


Figure 1.4 – Brayton-Joule ideal cycle [2]

Using the simplified first law of thermodynamics, that is, neglecting changes in kinetic energy and potential energy, the following expressions can be written.

The work of the compressor in terms of power:

$$W_c = \dot{m}_a (h_2 - h_1) \quad 1.1$$

The work of the turbine in terms of power:

$$W_t = (\dot{m}_a + \dot{m}_f) (h_3 - h_4) \quad 1.2$$

This results in a net work:

$$W_n = W_c - W_t \quad 1.3$$

The heat introduced per unit time can be written as:

$$\dot{Q}_{in} = \dot{m}_f LHV_f = (\dot{m}_a + \dot{m}_f) h_3 - \dot{m}_a h_2 \quad 1.4$$

Under the assumptions of the ideal cycle, it is possible to define the overall thermodynamic efficiency, assuming that the fuel flow rate \dot{m}_f is negligible compared with the air flow rate, as the ratio of net specific work to specific heat input:

$$\eta_{ideal} = \frac{w_n}{q_{in}} = \left(1 - \frac{1}{\beta^{\frac{\gamma-1}{\gamma}}} \right) \quad 1.5$$

The efficiency of the ideal cycle grows asymptotically as the ratio of pressures β increases. From the above, it is possible to make explicit the net specific work:

$$W_n = \eta q_{in} = (1 - \beta^{-\gamma}) \frac{R_g}{\beta} T_1 \left(\frac{T_3}{T_1} - \beta^\gamma \right) \quad 1.6$$

from which the dependence of work on maximum cycle temperature and compression ratio can be ascertained. In Figure 1.5, the efficiency and specific work as a function of β and t , the ratio of maximum temperature to minimum cycle temperature, are shown.

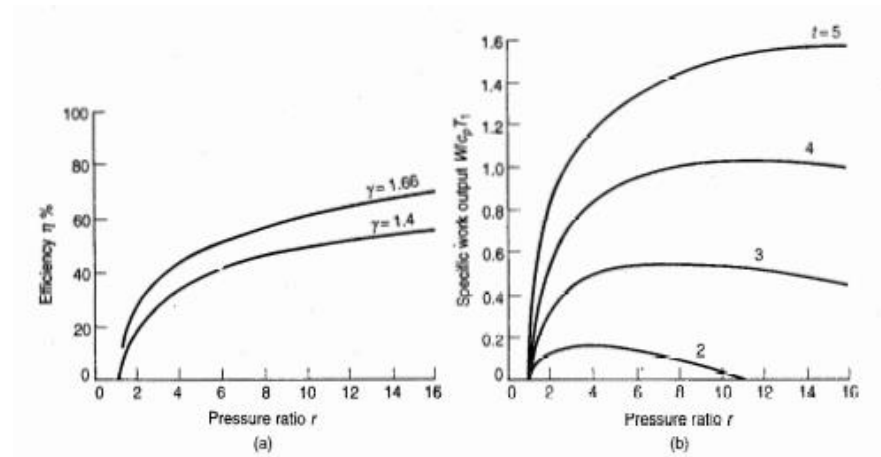


Figure 1.5 – Efficiency in function of the pressure ratio (a). Specific work output in function of the firing temperature and pressure ratio (b) [3]

In the real case there are losses that cause the efficiency to be lower than in the ideal cycle. Considering only the turbine and compressor efficiency losses, it is possible to write the overall efficiency as follows:

$$\eta_{cycle} = \left(\frac{\eta_t T_3 - \frac{\gamma-1}{\beta \gamma} T_1}{T_3 - T_1 - T_1 \frac{(\beta \gamma - 1)}{\eta_c}} \right) \left(1 - \frac{1}{\beta \frac{\gamma-1}{\gamma}} \right) \quad 1.7$$

Figure 1.6 shows the effect on overall cycle efficiency as the maximum cycle temperature increases. It can be seen that, as the pressure ratio increases, the efficiency increases for a fixed maximum temperature. Beyond a certain optimum value, however, there is a decrease in cycle efficiency. Having high β results in a reduction in the operating range of the gas turbine as we approach surge conditions. Under such operating conditions, the compressor becomes more sensitive to any deposits on the blades, leading to a drop in performance. In some cases, the compressor can stall, causing backfire and even major damage to the compressor blades and to the radial and thrust bearings of the gas turbine.

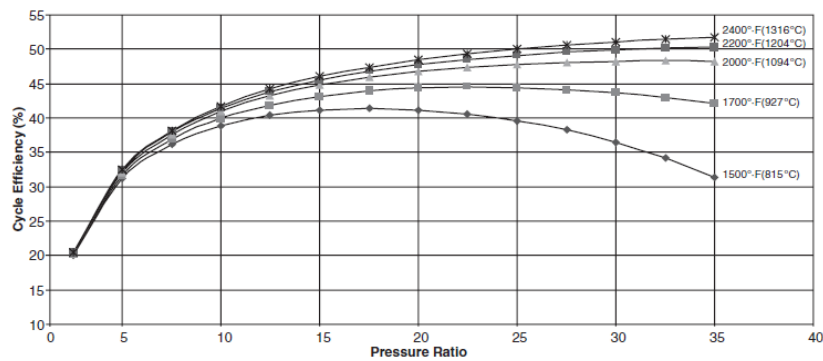


Figure 1.6 - Overall cycle efficiency as a function of the firing temperature and pressure ratio. Based on compressor efficiency of 87% and the turbine efficiency of 92% [3]

In addition to irreversibility losses in the compressor and turbine there are other sources of loss. These sources of loss are schematically shown in Figure 1.7.

- Transformations 2-3 and 4-1 are not isobars, but there are pressure losses at the intake, in the combustor, in the turbine inlet ducts, and downstream of the turbine (due to exhaust after-treatment systems, silencers, and any heat-recovery devices);
- Localized thermal losses in the various hot parts of the machine;
- Chemical energy losses due to incomplete fuel oxidation;
- Flow losses through seals;
- Losses related to cooling of high temperature parts;
- Mechanical losses: power absorption by ventilation, friction on bearings, auxiliaries, etc.

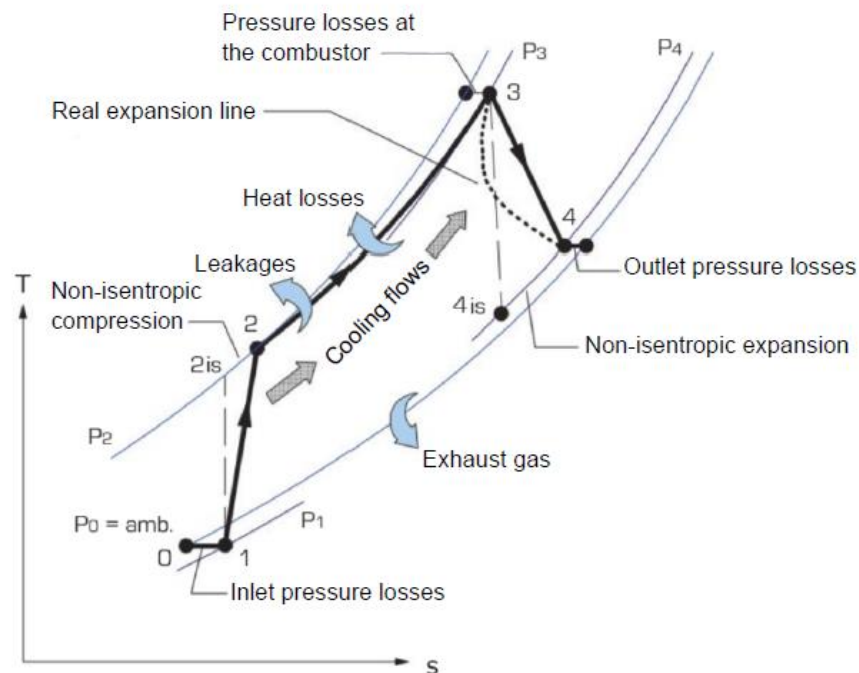


Figure 1.7 - Real open cycle of gas turbine in the T-s plane [3]

1.2.2 Gas Turbine Plant

In its simplest conception, the turbo gas plant consists of a multistage compressor, combustor, turbine, and electricity generator connected on the same shaft. The principle of operation is as follows: ambient air is drawn in and filtered in the intake duct, it is then compressed by the compressor stages. This results in an increase in pressure and temperature. The compressed air is then introduced into the combustion chamber, where it is mixed with fuel in such a way as to have controlled combustion. The combustion generates hot gases at high pressure that are fed into the turbine stages, which convert the energy into mechanical energy by turning the shaft. Finally, the electric generator converts the mechanical energy into electrical energy. The expanded air is conveyed to the exhaust system, which usually includes a gas post-treatment system to reduce emissions and possibly a heat exchanger to utilize the remaining energy. Indeed, it is pointed out that the thermal energy of the exhaust gas is about 60 percent of that of the fuel, which can be recovered for thermal uses, such as cogeneration, or to generate additional electricity by exploiting a steam turbine.

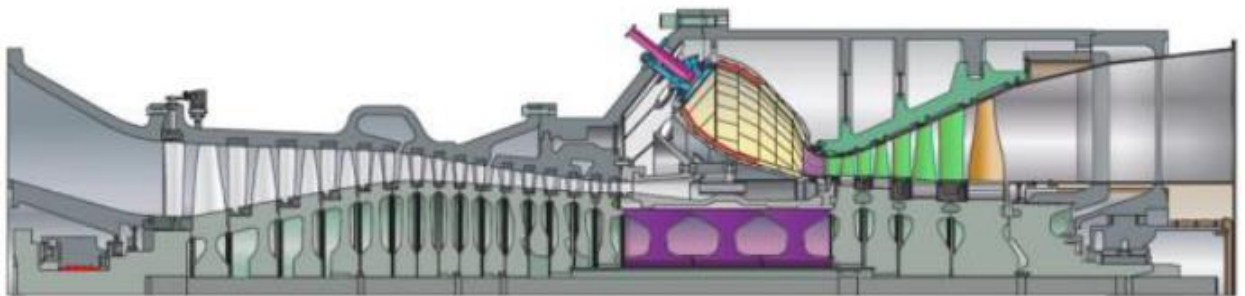


Figure 1.8 - Gas turbine section view (courtesy of Siemens)

Simple cycle gas turbines for industrial applications can be classified into the following categories:

1. *Heavy-duty o industrial*: these are the large units that can generate from 3 MW to over 500 MW in simple cycle with efficiencies ranging from 30% to 45%;
2. *Aero-derivative*: as the name suggests are units that originated for aeronautical application, which are adapted by replacing components, such as the fan and nozzle, with the power turbine. They generate from 2.5 MW to about 60 MW, with efficiencies ranging from 35% to 45%;
3. *Industrial Gas Turbine*: produce in a lower power range from 2.5 MW to 15 MW, with efficiencies of less than 30%;

4. *Small gas turbine*: are even smaller in size and produce from 0.5 MW to 2.5 MW, with efficiencies in the range of 15-25%;
5. *Micro-Turbines*: the last ones produce from 20 kW to 350 kW.

The first ones generally have a lower level of technology as they favor robustness and ease of maintenance in order to maximize the number of operating hours. Compression ratios are not high, 12-25, as they favor specific work produced at the same air flow rate. The second ones, on the other hand, have higher compression ratios as they promote efficiency over specific work. In general, aero derivatives offer greater flexibility and faster start-up times. Gas turbines can be found in different configurations: Single shaft or multi shaft (usually dual shaft), in the first ones all components are shrouded on the same generator shaft. In the dual shaft configuration, on the other hand, there is the hot gas generator, consisting of the compressor, combustor and turbine on the same shaft; and the power turbine shrouded on the generator shaft instead.

Generally, gas turbine powers and efficiencies are defined by ISO (International Organization for Standardization) conditions. The conditions are standardized for comparison and evaluation purposes, which include:

- Inlet air temperatures: 15°C;
- Atmospheric pressure: 101.325 kPa;
- Relative humidity: 60%;

In fact, atmospheric conditions can have important effects on power production and efficiency. A change in pressure, even a modest one, results in a change in the mass flow rate of the cycle, and thus a change in power output. In contrast, there is no effect on efficiency as the cycle moves to lower isobars at the same temperatures. A change in ambient temperature has significant effects on gas turbine performance and can affect several aspects of its operation. Mass flow varies with specific volume and thus inversely with temperature. This results in a change in the compression ratio, which decreases if the ambient temperature increases, resulting in a higher end compression temperature. Since the maximum cycle temperature is fixed, less fuel can be introduced, but since there is a lower pressure ratio available in the turbine, less work is obtained. This results in a reduction in efficiency.

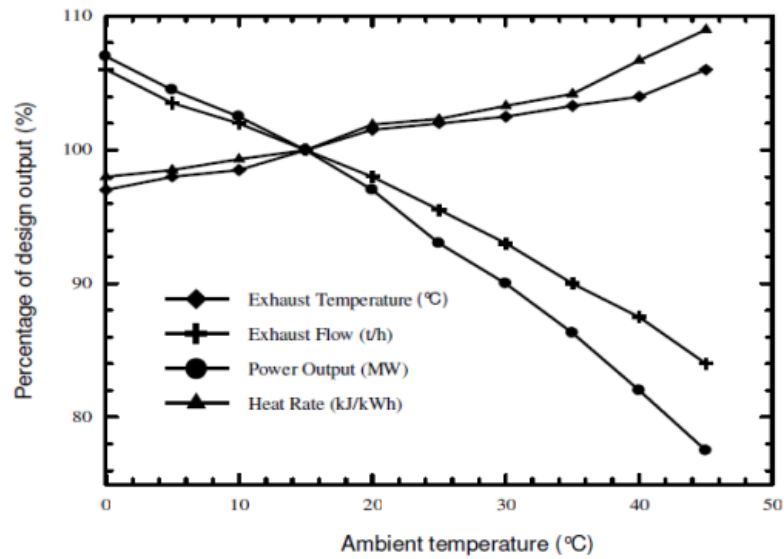


Figure 1.9 - Influence of ambient temperature on gas turbine performance parameters [4]

To mitigate the effects of ambient temperature, the plant has appropriate devices within the intake duct. In fact, in addition to the filter, which is necessary in order to reduce the presence of external objects in the airflow, there are also heat exchangers in the intake duct, such as a heater used to prevent ice formation on the compressor blades at low temperatures and a cooler to mitigate high temperatures instead. In addition, there is also a fogging device that uses the enthalpy of vaporization of injected droplets to bring down temperatures.

1.2.2.1 The compressor

The compressor of a gas turbine is generally a multistage axial compressor; exceptions are limited to small power machines, which use one or more stages of centrifugal compressor. Axial turbomachines have the advantage over centrifuges of being able to discharge higher volumetric flow rates with higher efficiencies at the cost of having lower compression ratios for each stage. Unlike the turbine, the compressor imparts an adverse pressure gradient, so it works under more sensitive aerodynamic conditions and consequently has significantly more stages. This results in less curved blades in the case of the compressor to avoid stall. Figure 1.10 shows the characteristic map of an axial compressor. This map is defined on the parameters derived from the dimensional analysis, which are: the reduced flow rate, the reduced rotational speed, and the pressure ratio. It can be seen that there is an upper limit defined by the surge line and a lower limit defined by the choking line. Surge is a form of flow instability that flows back to the inlet section of the compressor causing strong vibrations that can lead to blade breakage. Choking, on the other hand, occurs when flow velocities are close to the speed of sound; this results in a blocked flow condition from which it is difficult to move. Another problem is that of stalling, which is due to fluid vein detachment due to excessive incidence of flow on the compressor blades. This is associated with a lower flow rate than the design flow rate at the same rotational speed. Fluid vein

detachment results in a deflection of flow that goes to the other blades, causing a cascading effect called rotating stall. Since gas turbines are constrained in their rotational speed by the grid frequency (50 Hz in Europe) this problem is obviated through the use of Variable Stator Vanes at the inlet of the compressor. Such a system is called Variable Inlet Guide Vanes (VIGV) and allows regulation of flow rate and thus power without the need to vary rotational speed.

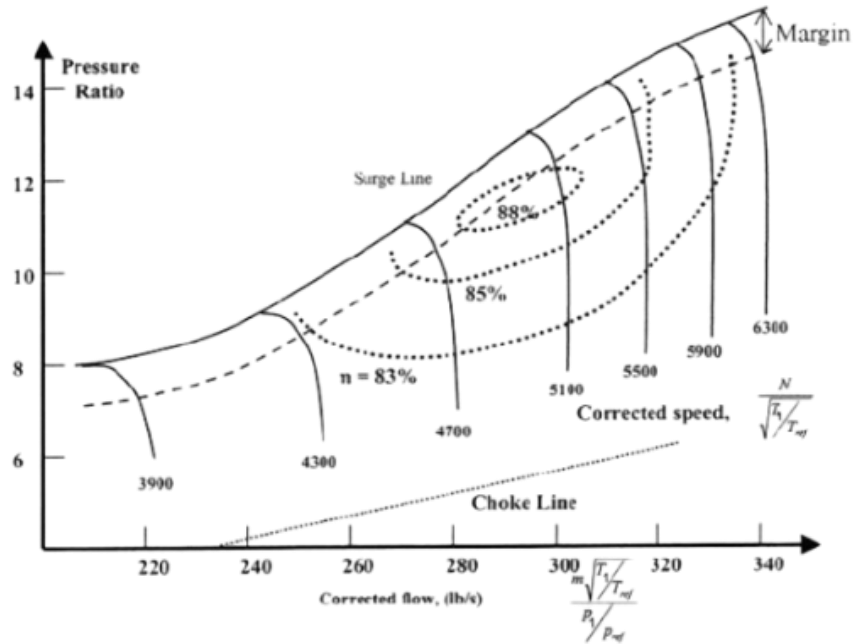


Figure 1.10 – Compressor performance map [5]

Where the corrected flow rate shown in abscissa is defined as follows:

$$\dot{m}_{corr} = \frac{\sqrt{\frac{T_1}{T_{ref}} \dot{m}}}{\frac{p_1}{p_{ref}}} \quad 1.10$$

While the corrected rotational speed:

$$N_{corr} = \frac{N}{\sqrt{\frac{T_1}{T_{ref}}}} \quad 1.11$$

Where T_{ref} and p_{ref} are the reference conditions defined by the manufacturer. In figure 1.10, the iso-performance curves can also be seen. While Figure 1.11 shows the effect of VIGV on the compressor map. The curve shifts to the left as the VIGV closes.

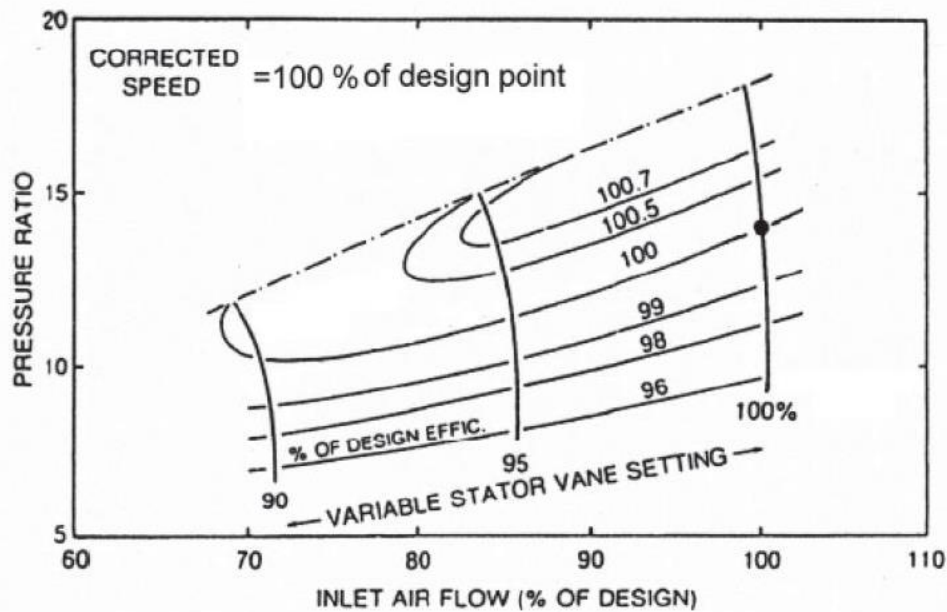


Figure 1.11 Effect of the VIGV on the compressor map [5]

The losses that characterize compressors can be distinguished into internal and external losses. The first ones are associated with the thermodynamic transformation that changes the fluid state and can be expressed through polytropic efficiency. These are mainly caused by fluid-dynamic losses internal to the machine. While external losses are for example friction losses and mass losses to the outside. Another characteristic parameter of the compressor is the isentropic efficiency, which will be discussed in more detail in the following chapters.

Some of the evolving flow in the compressor is bled through the secondary air systems (SAS) in order to carry out turbine cooling given the high temperatures.

1.2.2.2 The combustor

The combustor is responsible for increasing the temperature of the air leaving the compressor by transforming the chemical energy of the fuel. The maximum temperature it can reach is set by the technological state of the machine and the strength of the materials. Over the years, the temperature has risen due to the development of technologies that can cool components subjected to high thermal stresses. Because air reaches the chamber at high temperatures due to compression, and because the maximum temperature is fixed, there is an overall poor combustion. In fact, the dilution ratio is between 2.5 and 3.5 in the turbo gas since otherwise too high temperatures would be reached. The main goals of combustors are: low total pressure losses, high combustion efficiency, flame stability, output temperature as uniform as possible, low exhaust emissions, longevity, and ease of maintenance. The problem of ensuring efficient combustion while having an overall poor mixture is solved by a combustion strategy involving two different zones. First, the combustion chamber features a diffuser to reduce the velocity of the incoming air, promoting lower pressure losses and greater flame stability. Inside the combustor, about 20 percent of the flow rate is distributed

to a primary zone where fuel injection and thus combustion under stoichiometric conditions takes place. Dopo di che la restante parte viene fatta bypassare attraverso un liner che la ridistribuisce in una zona di diluizione, in cui si riducono le temperature e si uniformizza il profilo di temperatura. After that, the remaining portion is bypassed through a liner that redistributes it to a dilution zone, where temperatures are reduced and the temperature profile is equalized. That liner is nothing more than a perforated cylindrical container, which protects the outer case from high temperatures and is cooled through different techniques by the flow rate that has bypassed the primary zone. For good combustion efficiency to occur, it is important that the time through the primary zone is equal to the time required for complete combustion. Among the most important parameters is also the total pressure drop, which is intended to be minimized at the design phase. These losses can be divided into hot losses and cold losses. Cold losses are those mechanical losses due, for example, to viscosity and turbulence. Hot losses, on the other hand, are those losses due to the fact that there is heating of the gases due to combustion, which generates convective motions and thus losses.

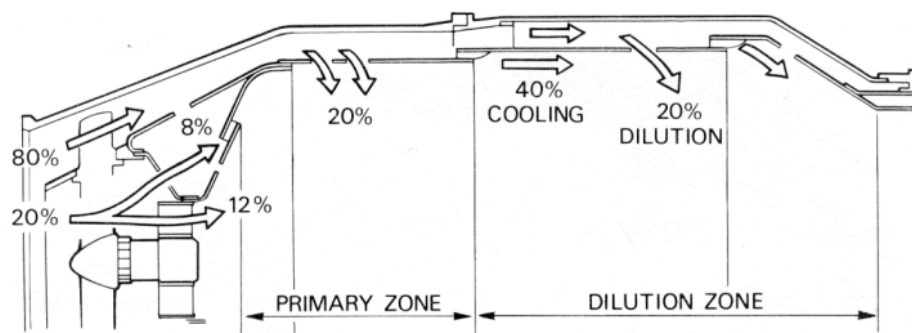


Figure 1.12 - Combustion chamber mass flow distribution [6]

There are three main types of combustors that characterize the geometric allocation, and they are:

- *Annular combustor*: features an annular-shaped case and liner, which compose a ring with multiple injection zones. It is the most compact geometry with lower pressure losses generally used for aircraft engines;
- *Canular combustor*: It consists of several circularly arranged tubular combustion chambers, which are connected by pipes to ensure uniform pressure distribution;
- *Can annular combustor*: is a midway of the previous ones in that it has a series of tubular liners arranged within an annular case;

Over the years, research has led to the development of new technologies in order to reduce pollutant emissions from these systems by introducing dual-stage combustors that can adapt to load variations through the use of a pilot stage, which is always in operation, and the main

stage, which is used when high power is required in combination with poor combustion premixing systems to reduce nitrogen oxides (NO_x).

1.2.2.3 The turbine

The turbine allows thermal energy to be converted into mechanical energy and given the high thermal and mechanical stresses to which it is subjected, it is the most critical component of the plant. There are several types: radial, axial and mixed. The most widely used in power generation is the axial turbine, which has stator blade and rotor blade. Because the transformation performed is an expansion, it is less affected by fluid dynamic issues, so the pressure drop can be achieved through the use of fewer stages than compressors, using larger deflections for the turbine blades. There are two types of turbines: the action turbine and the reaction turbine. In the first, all the enthalpy jump of the stage occurs in the stator; in the second, the enthalpy jump is divided between the rotor and stator according to the degree of reaction, a parameter of the stage. The first stages tend to be action stages, so the stator behaves like a nozzle and the rotor uses the kinetic energy of the flow to convert it into mechanical energy by the rotation of the blades with respect to the axis. The last ones, on the other hand, have reaction degree R equal to 0.5, so the expansion is split in both stage arrays. Figure 1.13 shows the velocity triangles, which describe how the work exchange takes place. Over the years, this component has been taken more and more to the limit, as efforts have been made to maximize the maximum temperatures of the cycle to improve efficiency and the specific work produced. Because the temperatures reached in the turbine are well above the maximum temperature supported by the best metallic materials, cooling technologies and materials have been developed that allow the blades to survive such high thermal and mechanical stresses.

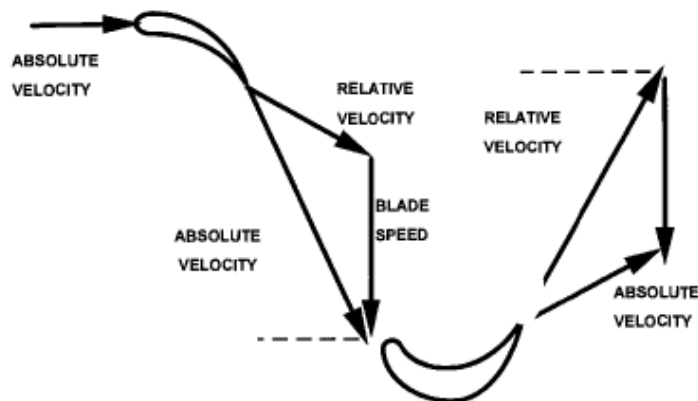


Figure 0.13 - Velocity triangles for design operating point [7]

Since there is the presence of a blade cooling system, there are different definitions for the maximum characteristic temperatures of the gas turbine. In fact, the following characteristic parameters are defined in the power generation world:

- T_{hg} : represents the temperature of hot gases at the combustor outlet, but given the very high temperatures, it is not possible to measure;
- T_{SOT} : is the temperature evaluated after the first stator array from the balance of the hot gas flow rate with the cooling flow rate conveyed to the stator;
- TIT_{ISO} : is the parameter par excellence used to characterize gas turbines. This parameter is calculated according to the ISO standard, from the hot gas balance with the total cooling flow rate.

Over more than 60 years, development has led to increasing the turbine inlet temperature to as high as 1,500°C. This has been made possible through the development of cooling technologies that take advantage of the air bleed from the compressor, which is conveyed through secondary air systems into the turbine zone. In addition to cooling the blades, it also serves to preserve the turbine disk and seal the gap between the rotor and stator so that secondary flow losses are significantly reduced. Figure 1.14 illustrates the SAS.

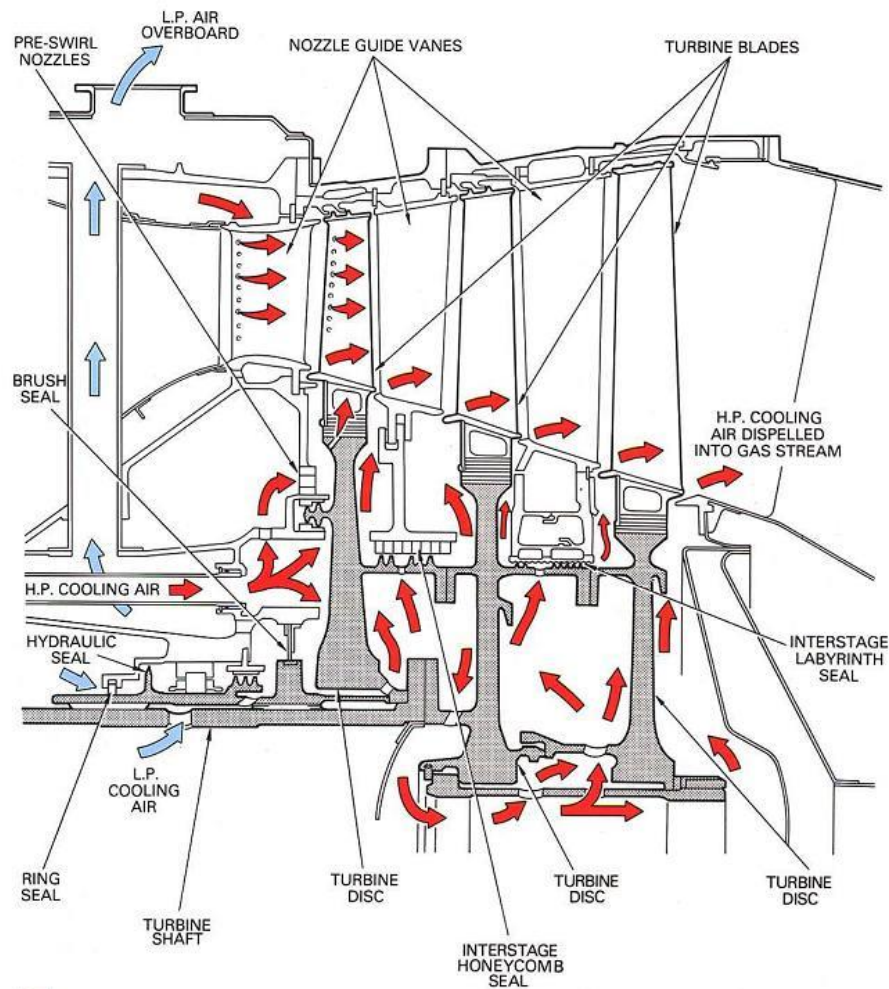


Figure 0.14 - Secondary air flow path in turbine [7]

Regarding cooling techniques, the main ones are obtained by forced convection, film cooling, jet impingement and transpiration cooling. It is possible for these technologies to be used in combination. Forced convection is achieved by conveying air inside the blades, and through turbulators the heat transfer coefficient is increased. Film cooling is a technique that through appropriate holes in the blade allows a protective film to be created on its profile. Jet impingement is a system that consists of creating a high-speed jet of air that hits the walls at greatest risk of overheating, usually the leading and trailing edge of the blade. Finally, the last technique takes advantage of porous walls that allow air from inside the blade to pass through to reduce its temperature. Such techniques can be observed in Figure 1.15. In terms of materials, on the other hand, superalloys have been developed that can resist creep and cyclic loads. With high cost and time, it is possible to obtain monocrystalline blades. Ceramic materials are not suitable for thermal transients especially when used for moving organs. Protective coatings have therefore been developed that can act as a thermal barrier and ensure the integrity of the blades against chemical attack. Such a thermal barrier is capable of providing temperature abatement of up to 100 °C and is composed of an outer ceramic layer, with an expansion coefficient equal to that of metal, and an inner metal layer.

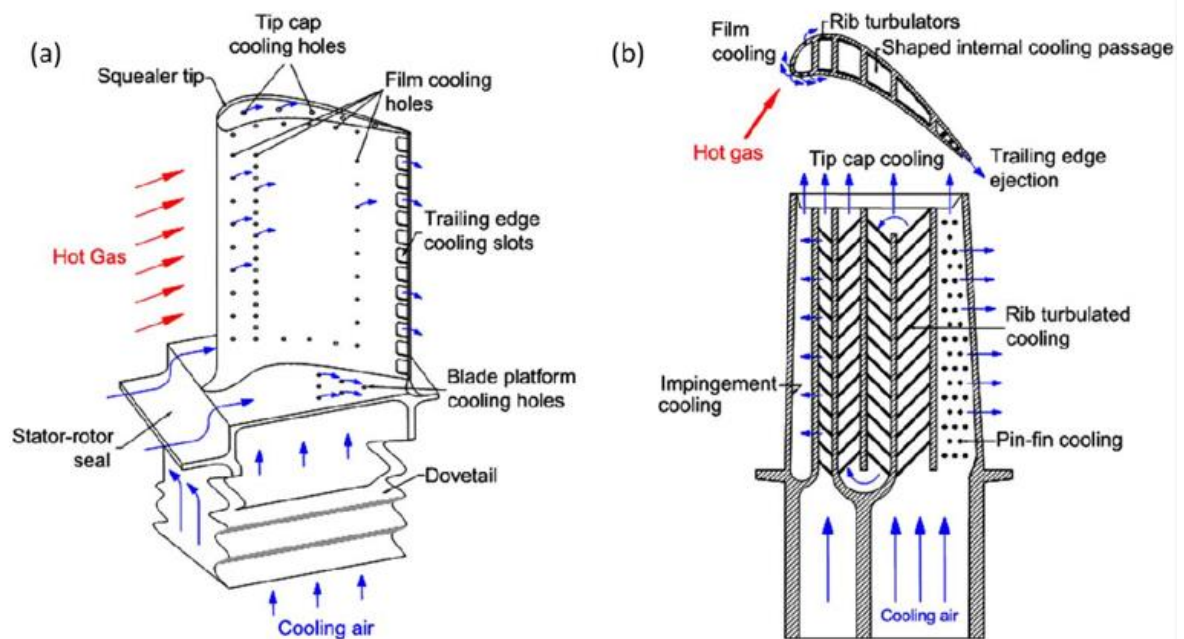


Figura 0.15 - Turbine blade cooling [7]

The effect of such cooling clearly affects the thermodynamic transformation and thus its efficiency. Mixing has three important effects, which are: a decrease in the temperature of the gases that will continue in the expansion and thus a reduction in the extractable work, the injected air having less velocity absorbs momentum from the gases, and also at the mixing point there are perturbations in the flow that increase its fluid dynamic losses.

Fluid dynamic losses are also significant, in fact, therefore there is a positive pressure gradient, the turbine stages have high aerodynamic loads in order to reduce the number of

stages. Among the main sources of losses is the boundary layer formed at the endwalls, which going to interact with the pressure gradients goes to form vortices within the palar canal. The presence of tip clearance, which is necessary to make it possible for the blades to rotate within the casing, causes vortices to be generated at the apex that go to dissipate energy and distort the flow. There are also profile losses and leakage losses between the rotor disk and the casing. These losses, together with those due to cooling go to affect the performance of the component.

In the same way as the compressor, it is possible to construct the turbine map, which has the same parameters but which refer to the turbine input conditions. Figure 1.17 shows the characteristic map of a turbine. Which shows in abscissae the pressure ratio and in ordinates the reduced flow rate. It can be seen that for any given reduced speed it is not possible to exceed a given reduced flow rate. This limitation is due to choking conditions. Generally, the design point is near the choking condition where the maximum isoentropic efficiency is obtained.

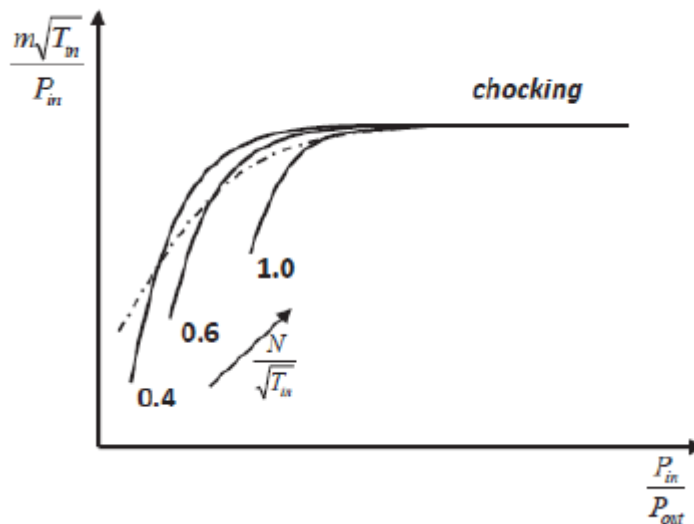


Figure 1.16 - Turbine performance map [5]

Turbine outlet temperature, referred to as TOT or TAT, is a crucial parameter in gas turbines because it reflects the operating conditions of the system and directly influences overall performance. This temperature depends mainly on the temperature of the combustion gases entering the turbine and atmospheric pressure. Considering that the gases leaving the turbine can retain a considerable amount of thermal energy, it is possible to exploit this residual resource to improve system efficiency. This is done using combined cycles or cogeneration systems, where the waste heat can feed heating processes or generate steam for industrial or heating purposes. This integration of heat recovery systems maximizes overall energy efficiency and reduces the environmental impact of industrial operations and power generation. Since exhaust gases have high kinetic energy, it is necessary to use a diffuser at

the turbine outlet, which allows it to be converted to static pressure, allowing acceptable flow conditions for the recovery and emission reduction systems that follow this component.

1.2.3 Combined Cycle Plant

A combined-cycle power plant is a highly efficient system for generating electricity that combines two different thermodynamic cycles: a gas turbine cycle and a steam turbine cycle. This integration allows additional energy to be extracted from the waste heat of the gas turbine cycle, resulting in significantly higher overall efficiency than conventional single-cycle power plants. Hot exhaust gases from the gas turbine are directed to a heat recovery steam generator (HRSG), where they transfer their thermal energy to water, generating steam.

The steam produced in the HRSG is then fed into a steam turbine, where it expands and moves a second generator to produce additional electricity. This combination of gas turbine and steam turbine cycles maximizes fuel energy utilization, as waste heat from the gas turbine cycle is effectively converted into useful energy through the steam turbine cycle. It is also possible that there may be an afterburner to increase the thermal power available to the HRSG, in which case it is called a fired cycle. The gas cycle is defined as the top cycle and the steam cycle as the bottom cycle since it underlies the former.

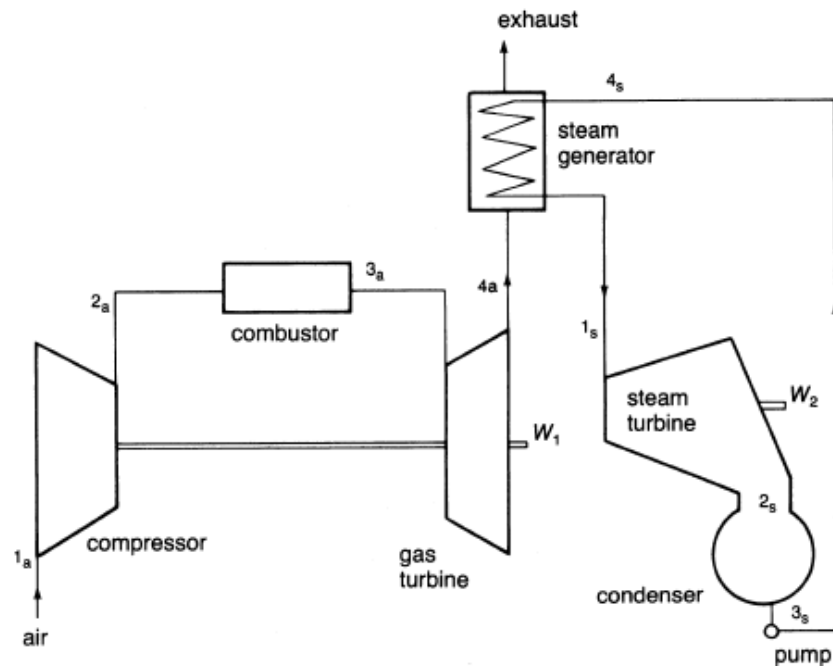


Figure 1.17 - Brayton-Rankine combined cycle [3]

The recovery boiler is the location of heat transfer between exhaust gas and the bottoming cycle fluid. Since the fluid is water and therefore subject to phase transition, a special boiler architecture is required. In its simplest version there is a single pressure level, but it is also possible to find HRSGs with two and three pressure levels. These pressure levels can be divided into high, medium, and low pressure, depending on the specific layout and design

of the HRSG. Each pressure level is connected to different sections of the turbine. Having multiple pressure levels allows for better utilization of the heat available in the boiler, increasing operational flexibility and optimizing overall efficiency.

In a single-level cycle, the boiler involves three operations: the heating of liquid water from the feed pump, the evaporation of water, and finally the superheating of steam. These steps take place in different sections of the boiler named economizer, superheater and reheater. Once the steam is generated, it is conveyed into the turbine and expanded until it reaches a saturated steam condition and thus is recirculated in the condenser. Figure 1.18 shows the thermodynamic cycle of the combined plant.

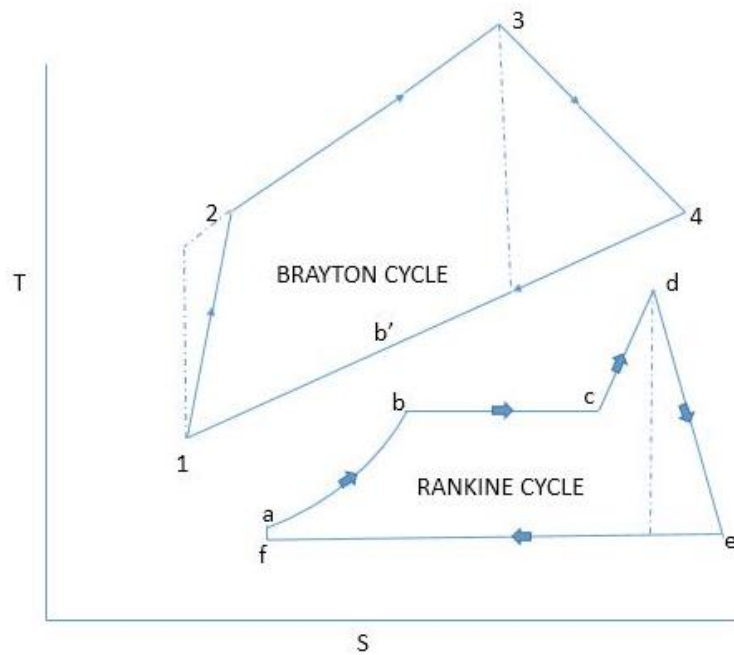


Figure 1.18 - Overall thermodynamic cycle

The presence of the HRSG goes to affect losses at the outlet and affects the system load transients, as the boiler is sensitive to thermal transients.

After discussing the fundamentals of gas turbines, it is essential to delve into the mechanisms of their degradation that motivate the need for monitoring.

1.3 - Gas Turbine Monitoring

1.3.1 Motivation

Gas turbines are exposed to thermal and mechanical stress conditions that cause their components to degrade. The degradation goes to affect the engine's operations causing a

decrease in performance and a consequent increase in exhaust emissions. Each component is characterized by different issues, which affect the behavior of the gas turbine locally and globally, and is subject to causes of failure. Monitoring makes it possible to assess the state of degradation of the machine and check for anomalies due to failures, giving the opportunity to intervene before a forced shutdown. With active monitoring, it is possible to extend the life of the machine and ensure high performance for the customer. Therefore, it is necessary to install on-site instrumentation in order to have real-time feedback of turbo gas performance. The histogram in Figure 1.18 shows how a reduction of up to one-third in operation and maintenance costs can be achieved by moving from corrective maintenance, based on fault intervention, to predictive maintenance, based on active engine diagnosis.

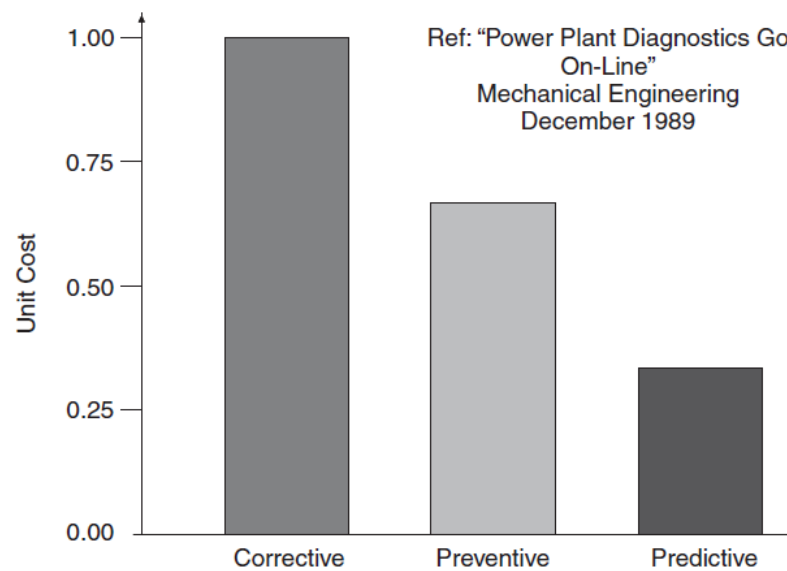


Figure 1.19 - Costs in function of the maintenance techniques

In many cases, power plant contracts include terms governing the responsibility of the manufacturer if the performance of the plant fails to meet certain agreed standards. These clauses may include provisions for cost reimbursement or other forms of compensation if the plant does not perform as promised. Sudden failures create serious repercussions for the customer, who will not be able to produce the energy he or she sold in the market and will have the plant shut down for an extended period of time.

1.3.2 Gas Turbine degradation

Degradation is a process of deterioration of gas turbine performance due to various factors, internal and external to the engine. These can include particle deposits, corrosive actions by chemical elements, and wear and tear from thermal and mechanical stress. Some of these phenomena are discussed in more detail below.

1.3.2.1 Fouling

Fouling consists of the accumulation of deposits on the compressor blades, which is aerodynamically sensitive to vane shape variation and surface roughness. Shape variation can cause an increase in blade load resulting in an increase in boundary layer development, furthermore, roughness causes an increase in profile losses. Agents responsible for fouling include industrial pollution, the presence of saline in the air, not particularly clean water from evaporative coolers, the presence of chemical fertilizers in the air, and more. This issue causes a decrease in flow rate, resulting in the emergence of flow incidence on the blades, which causes the operating point on the compressor map to move close to the surge line, reducing the compressor's work exchange efficiency. To mitigate this problem, the only possible actions are: using a filter at the suction of the turbomachinery and performing compressor flushing. Washing differs into two types, depending on whether it takes place while the machine is on (On-Line wash) or off (Off-Line wash). It is important that both are performed in the maintenance cycle to keep efficiency high.

1.3.2.12 Foreign Object Destruction and Domestic Object Damage

The presence of foreign objects inside the gas turbine can cause significant damage to the engine. Such objects may come from the intake duct or from the detachment of machine parts that are carried into the gas path. They are referred to as FOD (foreign object destruction) and DOD (domestic object damage), respectively. This results in irreversible damage to the blades that impairs the efficiency of the machine leading to costly repairs. The effect can be difficult to distinguish from fouling, so it requires in-depth analysis of measurements and performance. The main signs can be highlighted on the isentropic efficiency of components and flow capacity. Appropriate filters should be used to reduce the effects of FOD, and periodic inspections should be carried out for DOD.

1.3.2.3 Tip Clearance

The tip clearance required for the rotor to rotate freely causes efficiency losses and reduced flow capacity as the flow is free to pass. Due to the pressure difference between pressure side and suction side an apex vortex is to be generated which affects the flow motion field causing further losses. Due to the thermal transients of the gas turbine it is possible for the rotor to rub against the outer case causing the gap to increase and consequently the losses. The observable effect is similar to fouling but is much more pronounced.

1.3.2.4 Erosion

Erosion is due to the presence of solid particles in the flow such as sand or metal debris that going to impact the blades go to erode the blade surfaces. The change in blade shape affects airflow distribution and pressure, compromising performance. The result is a decrease in the operational life of the blades, and therefore a greater frequency of maintenance work. It is therefore necessary to monitor the situation through visual inspections or performance analysis to avoid incurring more serious damage.

1.3.2.5 Corrosion

Corrosion is a phenomenon that takes place through chemical reactions between some contaminant, which passes through the gas path, and component surfaces. Corrosive substances can come from ambient air, injected water/steam, or fuel.

1.3.3 Problem definition

The operation of the plants relies on a control system that is essential to ensure the proper functioning of these machines. It regulates the speed of the turbine, monitors and manages the temperatures of exhaust gases and critical components, controls the combustion process, protects the turbine from overloads and failures, adjusts the power produced according to energy demand, and manages pollutant emissions. In essence, the control system ensures that the gas turbine operates safely, reliably, and efficiently under all operating conditions. It requires robust instrumentation to perform this task, which for practical and cost reasons cannot always be comprehensive. In fact, some parameters may be obtained indirectly using other measurements. Such instrumentation is also used to perform performance tests during commissioning and during the life of the plant, to demonstrate that the performance is as guaranteed to the customer.

It is such measurements that are used for the remote monitoring system. In fact, thanks to the use of the Internet, it is possible to access the measurements that are saved within a data base. In this way the manufacturer is able to access the measurements in real time and through them perform heat balances, which provide information on the performance of each component. A virtual model of the gas turbine must be used to perform these calculations. In the specific case presented in this paper, the model is built on in-house software, acquired from *Alstom*, called *Alpeg*. Within the software, each component is modeled through equations that describe its behavior, such as flow balance equations and energy balance equations. In addition, the performance parameters to be estimated are defined for each component. The equations describing each component will be discussed in more detail in the following chapters. Figure 1.19 illustrates the construction of the turbine model, which must be customised to reflect the current state of the plant and include each component interconnected with the others.

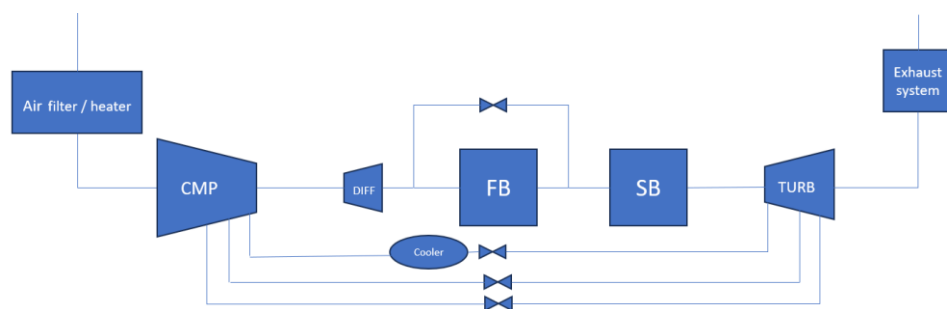


Figure 1.19 - GT modelling

For components such as the turbine and compressor, characteristic maps are implemented from which it is possible to evaluate parameters that are not measured or are considered as unknown during calculations. In fact, different types of heat balances can be carried out depending on the measurements that are considered reliable in order to be able to calculate those that are considered unreliable or to carry out a simple verification. In addition, assumptions are made about certain efficiencies, such as that of the transformer and bearings. Since the turbo gas is subject to degradation, the model and thus the characteristic equations of each component will have to be updated periodically. Similarly, in case physical improvements are implemented to the components.

Among the main problems that this project aims to solve is the reliability and accuracy of the measurements. In fact, it is possible that they can be wrong for several reasons: sensor failures due to sensor degradation, incorrect calibration of the instrument, presence of electromagnetic interference, failures due to the striking of objects passing through the gas path or sediment of liquid or solid particles on the sensitive part of the instrument. Pre-processing of measurements is therefore a fundamental part of the monitoring system because it allows for reliable calculations and thus more accurate engine diagnostics. Although a processing system was already available it was often fallacious and not exploitable for monitoring on a daily basis. In fact, it through statistical analysis avoids any bias within the redundant measures, being fragile compared to nonredundant measures. In Figure 1.20 and 1.21 it can be seen how it works on the measurements of the single physical quantity measured. To avoid any completely wrong measurements it performs a check on the absolute value by verifying that it is within predetermined limits, which should be as general as possible. While through a user-defined tolerance defined in percentage or absolute value it allows avoiding bias on redundant measurements. This process is achieved by the *Measurement Data Preparation* tool (MDP), it prepares the values to be sent to the software used for calculations by assigning pre-processed values of the measurements to the parameters implemented on *Alpeg*.

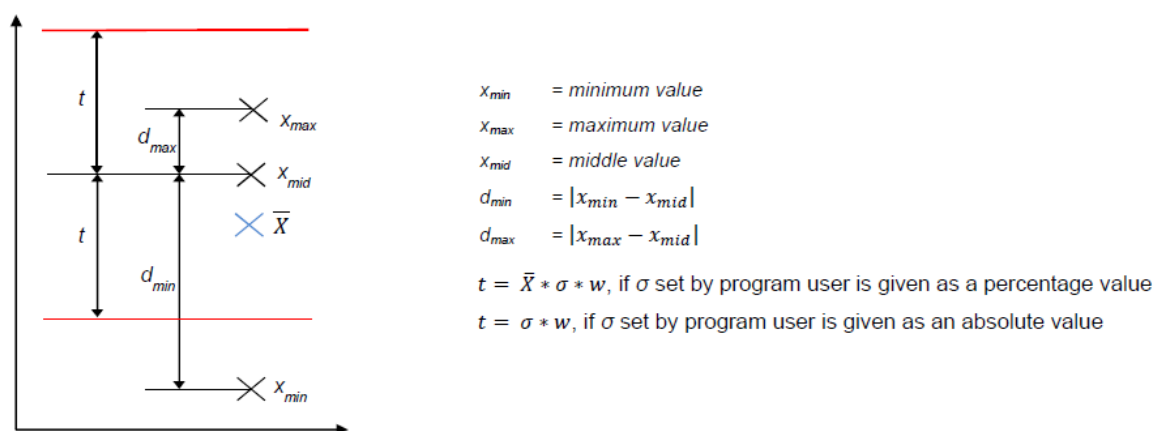


Figure 1.20 - Measurement Data Processing on redundant measures

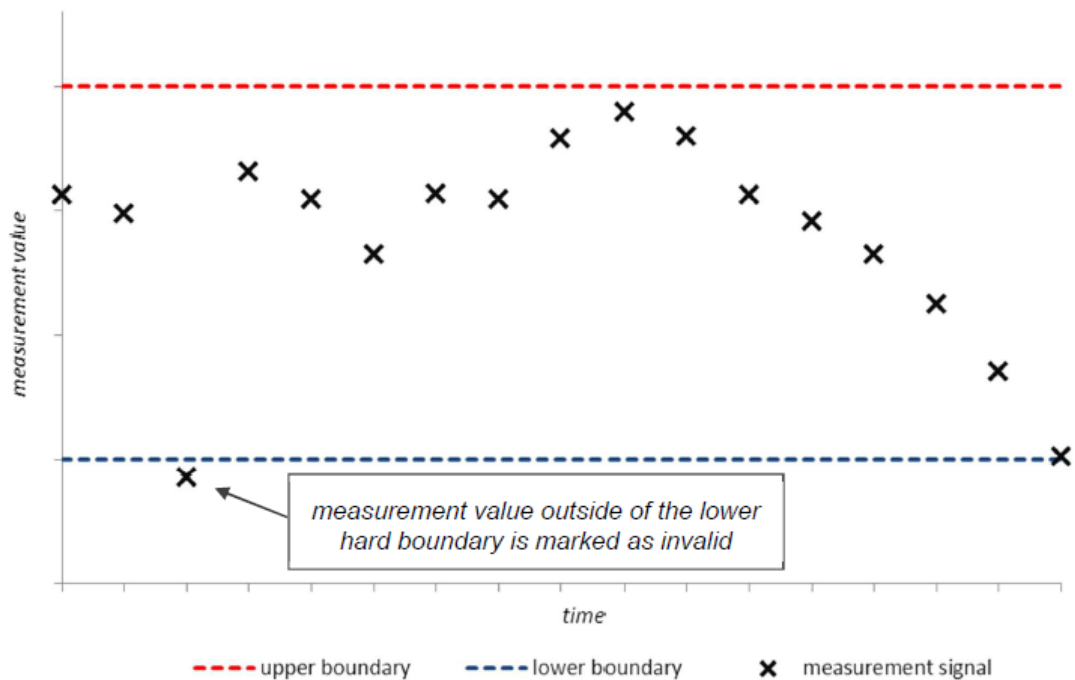


Figure 1.21 - Measurement Data Processing tool

Therefore, the limitation of such a processing system can be deduced since it cannot control the measurement against the target value representing the operating condition. To resolve this situation, a system capable of performing calculations on the model, using only a few fundamental measurements characteristic of the operating condition, and then comparing the results with the measurements.

For this purpose, it was necessary to implement an automatic code that initially, through an *Excel* file downloads the measurements from the plant database and saves them within specific folders. One of these folders contains the raw measurements. Another, on the other hand, contains the measurements on which to perform calculations on the model to obtain the reference values. For the last ones not to be wrong, it is necessary to check the reliability of the measurements on which the calculations are made, some of which are:

- The pressure drop in the intake duct;
- The pressure drop at the plant exhaust;
- The position of the VIGV;
- The ambient conditions: temperature, pressure and humidity;
- The chemical composition of the fuel.

On the pressure drops it goes to verify that they are not too far from the reference value corresponding to the operating condition. This reference value is calculated within the code, in which the characteristic equation of the component is implemented, which is described as a function of the temperature and the position of the VIGV, being proportional to the air

flow through the motor. Once what is described has been done, the code launches *Aleg* in *Synthesis* mode, allowing values to be obtained for comparison with the raw measurements obtained from the gas turbine. For each measurement the code goes to check the distance from the value predicted by the model in order to check for erroneous measurements. Once the processing is done, it is finally possible to obtain heat balances by running the *Alpeg* software in *Heat Balance* mode on the processed measurements.

When the details of measurement sampling have been defined, the end user of the code will be enabled to perform the process. This involves defining the start and end date and time of the sampling, as well as specifying the distance of the measurement points. Through a single click, the user can then access a database of reliable calculations that provide a description of the gas turbine status. The workflow of the monitoring package is illustrated in Figure 1.22.

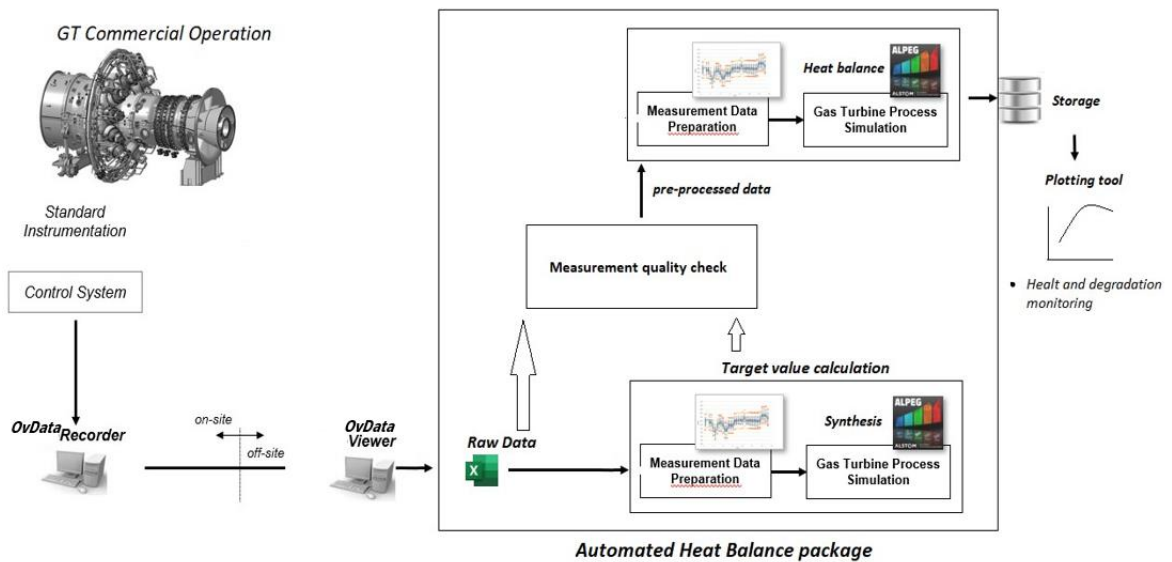


Figure 1.22 - Monitoring package workflow

2. Performance Monitoring tool

In this chapter, we will examine the method used to conduct the calculations required to evaluate gas turbine (GT) performance. We will begin by introducing the indispensable instrumentation that must be integrated within the turbo gas, allowing us to define the boundary conditions for each component modelled in the software. Afterwards, we will explore the main functions implemented within the software and conduct an analysis of the solver, highlighting its limitations and explaining its approach to solving the system of equations.

2.1 – Instrumentation

The instrumentation installed inside the engine is a requirement of the monitoring system. High-quality measurements lead to more reliable results and thus make monitoring possible. Among the main problems with the measurements is reliability and accuracy, which is the focus of this thesis work.

Generally, performance evaluations take place on predefined occasions. First of all, they are carried out after the GT has been commissioned to verify that the performance guaranteed to the customer is met. In addition, performance tests are also carried out following periodic inspections, after any damaged components have been replaced, and after cleaning the components through, for example, compressor washing and the use of strainers. On such occasions, the available instrumentation is likely to be higher than during normal commercial operations. The aim of the project is precisely to allow more frequent monitoring compared to performance tests, while trying to obtain high quality measurements using the instrumentation implemented for the control system. The main instrumentation that can be found inside the GT plant is shown below.

2.1.1 Pressure measurement

Pressure measurements are conducted using calibrated electronic transducers, such as piezoelectric and capacitive transducers, but analogue systems such as pressure manometers can also be implemented to calibrate the former. The selection of the type and number of instruments used for pressure measurement must be carefully considered, considering the magnitude and range of the measured value, the required accuracy, and the specific flow dynamics in the proximity of the sensor. It is imperative to pay particular attention to the positioning and installation of pressure instruments, in order to avoid additional errors caused by environmental conditions such as radiation, vibration, interference and the presence of leaks, which could increase the uncertainty of readings.

The main pressure measurements include the following:

- *Ambient pressure*: which must be measured in a location protected from any kind of interference.
- *Differential pressure at inlet*: pressure drop between ambient and gas turbine flange inlet pressure.
- *Compressor discharge/Combustor pressure (p_{k2})*: measurement of relative pressure at the combustor inlet.
- *Pressure in secondary air systems*: these measurements are carried out at the purge cavity and inside the pipes.
- *Exhaust pressure*: measurement of pressure at the gas turbine flange outlet. This measurement is used to calculate the exhaust static pressure loss.

It is possible that some pressure measurements are used to evaluate mass flow rates.

2.1.2 Temperature measurement

Temperature measurements provide very useful information on the efficiency of the engine and components. In fact, definitions of polytropic efficiency are based on temperature and pressure, and they are also necessary to verify that the engine is working within the limits of mechanical integrity. In addition, temperature is used to evaluate mass flows. Two main types are used for such measurements: resistance thermometers and thermocouples. As they are inserted inside flows, the measured temperature is likely to be a total temperature and must therefore be corrected if a static measurement is intended. A fundamental characteristic of such sensors is the transient response, which in the case of large thermocouples may not be negligible.

The main temperature measurements include the following:

- *Ambient temperature*: typically measured through redundant measurements to avoid non-uniform temperature distributions. It is in fact important that they are placed in protected locations.
- *Compressor inlet temperature*: This temperature is normally used for performance analysis because it is more reliable compared to the ambient temperature measurement.

- *Turbine exhaust temperature*: this is a fundamental parameter also used by the control system. Since there can be temperature non-uniformity at the exhaust, it is important that there are several sensors positioned circumferentially in this section.

The TIT temperature is not reported as there are no probes capable of supporting certain temperatures, furthermore, the temperature is highly non-uniform at the combustor outlet, therefore, it would be difficult to estimate a reliable average temperature.

2.1.3 Fuel measurement

The main measurements performed on gaseous fuels include density, composition, temperature, pressure, volume flow and the lower heating value (LHV). Through the pressure and temperature value, the density value can be traced. The chemical composition and the value of LHV can be assessed through the chromatograph. This information is used for both the control system and the monitoring system to carry out energy balances.

2.1.4 Mass flow measurement

Various types of instruments are available for evaluating evolving ports, such as venturi tubes, differential pressure gauges, anemometers and flow turbines. The choice of sensor depends on the specific measurement requirements and flow characteristics. It is important to select the most suitable sensor and calibrate it accurately to ensure precise and reliable flow measurements within the gas turbine system. These measurements are made inside the SAS piping and in the fuel supply lines.

2.1.5 Other measurement

In addition to these measurements, the following quantities are evaluated:

- *Ambient uumidity*: Measurement of the humidity of the ambient air entering the gas turbine, which is evaluated in the most appropriate section if humidifiers and heat exchangers are present. It can be measured directly using hygrometers or can be obtained indirectly using thermophysical tables.
- *Gross power*: through appropriate instruments supplied with the generator, it is possible to obtain the power fed into the grid.
- *Rotation speed*: by means of appropriate instruments such as encoders, it is possible to assess the shaft's rotation speed, which must be constant while respecting the mains frequency.

- *VIGV position*: this measurement is fundamental for the control system but also for the performance tool. To have a robust measurement, redundant sensors are used to evaluate the angle of the variable orientation stator blades.

2.1.6 General requirements

To obtain reliable calculations, it is necessary to have robust instrumentation that allows redundant measurements to be used as much as possible to avoid possible sensor problems. It is important that the measurement uncertainty is kept as small as possible for the same reasons. Figure 2.1 shows the maximum acceptable uncertainties according to the ISO 2314 standard for performance tests. To avoid systematic error, it is important that such instrumentation is calibrated periodically according to the manufacturer's instructions.

Some of the main causes that can lead to erroneous measurements include:

- *Sensor failure*: sensors used to measure critical parameters such as temperature, pressure and flow can break or become damaged over time, affecting the accuracy of measurements.
- *Fouling of the sensing element*: deposits of dirt, dust or combustion residue can accumulate on the sensors over time, reducing the sensitivity and effectiveness of measurements and causing errors in readings.
- *Presence of electromagnetic interference*: electromagnetic interference generated by other equipment or external phenomena can affect the sensor signal, altering measurements and compromising the accuracy of measured data.
- *Improper calibration*: Incorrect initial calibration or lack of periodic calibrations can lead to significant deviations from accurate measurements.
- *Mounting errors*: Problems during mounting or installation of the sensors can lead to incorrect positioning or faulty connections, impairing the effectiveness and accuracy of measurements.
- *Performance degradation*: over time, sensors may suffer performance degradation due to wear or corrosion of materials, resulting in long-term deterioration of measurement accuracy.
- *Transient inadequacy*: the presence of hysteresis can affect the accuracy and reliability of measurements, especially in control and regulation systems where a consistent and predictable response is required.

Individual instrument or parameter	Max. uncertainty	Remarks
Barometric pressure	$\pm 0.05 \%$	Instrument uncertainty
Air inlet temperature	$\pm 0.2 \text{ K}$	Instrument uncertainty
Relative humidity	$\pm 2 \%$	Instrument uncertainty
Electrical power metering	$\pm 0.2 \%$	Instrument uncertainty
Current transformer	$\pm 0.2 \%$	Equivalent to accuracy class 0.2S
Voltage transformer	$\pm 0.2 \%$	Equivalent to accuracy class 0.2S
Mechanical power (torque)	$\pm 1.0 \%$	Instrument uncertainty
Frequency / Shaft speed	$\pm 0.25 \%$	Instrument uncertainty
Gas fuel pressure	$\pm 0.25 \%$	Instrument uncertainty
Gas fuel temperature	$\pm 0.2 \text{ K}$	Instrument uncertainty
Gas fuel heating value	$\pm 0.5 \%$	Combined uncertainty of gas composition
Gas fuel mass flow	$\pm 0.5 \%$	Combined uncertainty of temperature, pressure, volumetric flow and gas composition
Oil fuel temperature	$\pm 0.2 \text{ K}$	Instrument uncertainty
Oil fuel heating value	$\pm 1.0 \%$	Combined uncertainty of laboratory analysis
Oil fuel mass flow	$\pm 0.5 \%$	Combined uncertainty of volumetric flow and temperature
Turbine exhaust temperature	$\pm 3 \text{ K}$	Instrument uncertainty
Inlet pressure loss	$\pm 50 \text{ Pa}$	Instrument uncertainty
Exhaust pressure loss	$\pm 50 \text{ Pa}$	Instrument uncertainty

Figure 2.1 - Maximum permissible uncertainties [8]

2.2 – Gas Turbine Model

To perform calculations on the Alpeg performance tool suite, it is necessary to construct a model of the gas turbine. This model is constructed by using a tool within the Alpeg tool suite, which, thanks to a graphic interface, allows all the components within the plant to be inserted and connected together. Each component is characterised by variables, parameters, the equations describing its behaviour and libraries containing characteristic maps of the same. In the construction phase, it is important to take into account that the number of unknowns must equalise the number of equations. To have a representative model, it is also necessary to integrate libraries containing the thermodynamic properties of the fluids flowing through each component. All of the above information defines the dataset, within which the variables can be assigned measurements and thus calculations such as heat balance and synthesis can be performed, which are described below. In the following discussion, reference will be made to the numbering shown in Figure 2.2.

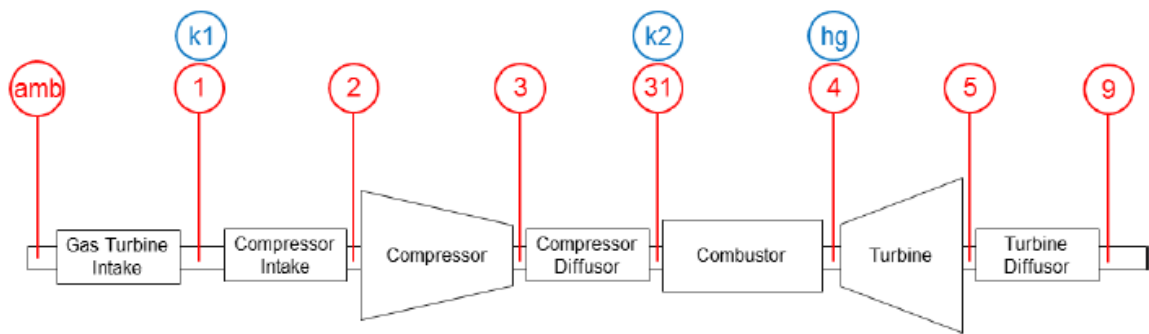


Figure 2.2 - Gas Turbine component numbering

2.2.1 Heat Balance

Heat balances are nothing more than energy balances on control volumes, taking into account all the heat and power entering and leaving the system. Figure 2.3 shows the control volume of the entire system, in a simplified version, with the associated energy exchanges, highlighting the values used as inputs in bold. The heat balance allows in this way the calculation of non-measurable parameters such as compressor inlet flow rate \dot{m}_{in} and hot gas temperature T_{hg} as well as performance related component parameters like the polytropic efficiency of the turbine.

In addition to the measurements required to perform the energy balance on the entire system, the figure also shows the measurements required to impose the boundary conditions of each component, such as the pressure and temperature measured in the SAS ducts or at the compressor outlet. The heat and mass balances are therefore shown below.

The composition of the dry ambient air is fixed. The enthalpy of the working fluid depends on the temperature (ideal gas assumption, therefore no pressure dependency) and working fluid composition. The working fluid composition dependency is not shown in the formulas for simplification. The fuel lower heating value LHV is calculated from the fuel composition. Because the gas composition at the exhaust is unknown and the enthalpy calculation from the exhaust temperature cannot be done in the first step always an iterative solution is required.

Observe the arrangement of the SAS system, which includes the MBH10 pipe as the first bleed system, the MBH20 pipe as the second compressor bleed system and the MBH30 pipe as the third bleed system. The latter system is divided into two sub-systems: one conveys the cooling flow to the rotor, which in turn cools the turbine's rotor blades and those exiting the compressor, while the other flow goes to the turbine's first stator vane. It is important to note

that this system is equipped with a water heat exchanger that helps to reduce the temperatures of the cooling flow.

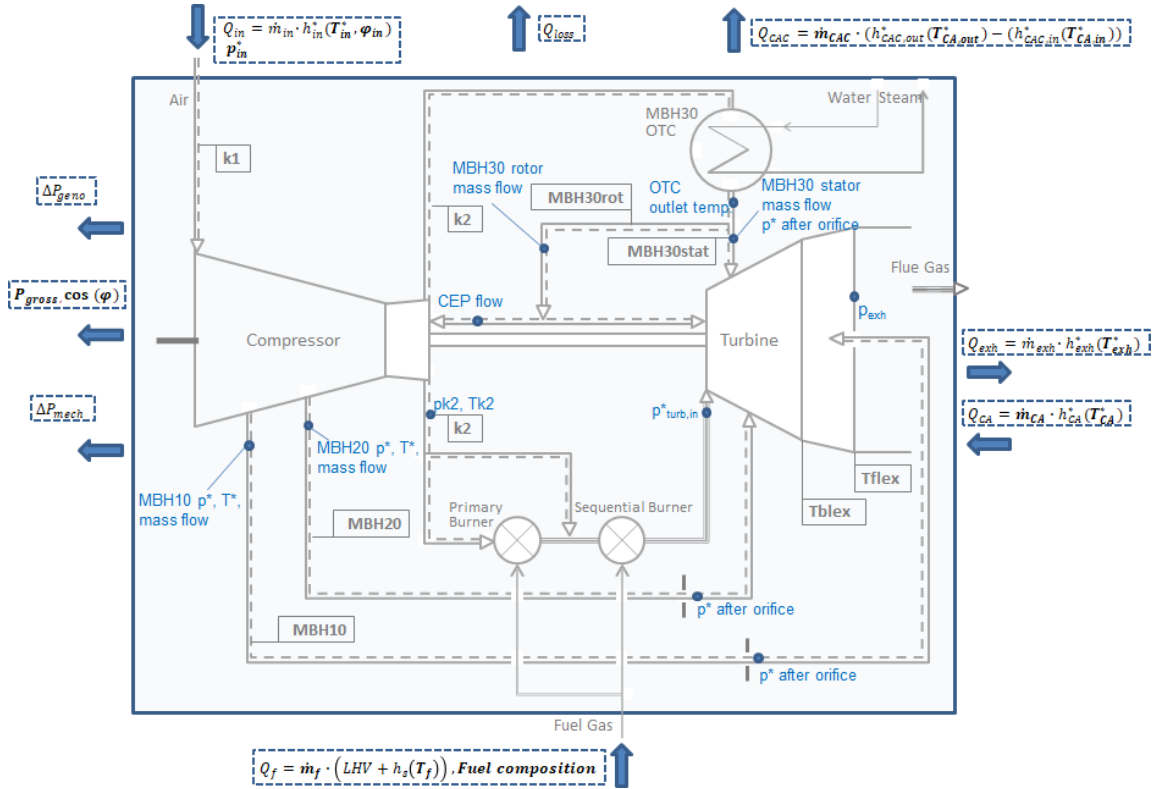


Figure - 2.3 Gas Turbine heat balance

The overall balance of the plant is described in the following relation:

$$Q_{in} + Q_f + Q_{CA} = Q_{exh} + Q_{loss} + abs(Q_{CAC}) + P_{Gross} - \Delta P_{geno} - \Delta P_{mech} \quad 2.1$$

Where the heat input refers to the input flow rate:

$$Q_{in} = \dot{m}_{in} \cdot h_{in}^* \quad 2.2$$

The heat associated with the fuel which takes into account the sensible enthalpy of the fuel as it is heated before being injected into the chamber is defined as:

$$Q_f = \dot{m}_f \cdot (LHV + h_s) \quad 2.3$$

The heat exchanged with the cooling water in the secondary air pipes are defined as:

$$Q_{CAC} = \dot{m}_{CAC} \cdot h_{CAC}^* \quad 2.4$$

$$Q_{CA} = \dot{m}_{CA} \cdot h_{CA}^* \quad 2.5$$

Exhaust heat is defined as:

$$Q_{exh} = \dot{m}_{exh} \cdot h_{exh}^* \quad 2.6$$

While the associated mass flow balance is as follows:

$$\dot{m}_{in} + \dot{m}_f + \dot{m}_{CA} = \dot{m}_{exh} \quad 2.7$$

In order to carry out the global balance, not all the necessary parameters are available; therefore, assumptions are required or the use of component maps is necessary. For example, for combustor radiation heat losses, an estimate can be made through this equation:

$$Q_{loss} = \epsilon_{loss} \cdot Q_f + (1 - \eta_{combustion}) \cdot Q_f \quad 2.8$$

Where:

- ϵ_{loss} is a coefficient expressing this loss.
- $\eta_{combustion}$ is the combustion efficiency which takes into account the fact that combustion may not be complete.

Mechanical losses are calculated from the mechanical efficiency assumptions:

$$\Delta P_{mech} = P_{shaft,1} \cdot (1 - \eta_{mech}) \quad 2.9$$

Instead, generator losses are evaluated through the characteristic of the component itself:

$$\Delta P_{geno} = f(P_{gross}, \cos(\varphi)) \quad 2.10$$

Consequently, the power available at the shaft minus mechanical losses and the gross electrical power are defined as:

$$P_{shaft,2} = P_{TU} - P_{CO} - \Delta P_{mech} = P_{shaft,1} - \Delta P_{mech} \quad 2.11$$

$$P_{gross} = P_{shaft,2} - \Delta P_{geno} \quad 2.12$$

Based on the above, the overall cycle efficiency can be calculated from the following:

$$\eta_{gross} = \frac{P_{gross}}{\dot{m}_f \cdot (LHV + h_s)} \quad 2.13$$

In addition to the global balance equations, there are equations describing the components. In order not to overload the paper, the main characteristic equations of the components are shown, which make it possible to assess the fundamental efficiencies to be monitored.

2.2.1.1 - Intake system

The pressure drop at the intake can be divided into the filter part and the silencer part.

$$\Delta p_{intake}^* = \Delta p_{filter}^* + \Delta p_{silencer}^* \quad 2.14$$

These components have a characteristic that can be scaled under conditions other than reference conditions; equation 2.15. It tends to be measured so it is an input to the calculation.

$$\Delta p_{intake}^* = (\Delta p_{ref,filter}^* + \Delta p_{ref,silencer}^*) \cdot \frac{\dot{m}_{intake}^2}{\dot{m}_{ref,intake}^2} \cdot \frac{T_{intake}^*}{T_{ref,intake}^*} \cdot \frac{p_{ref,intake,in}^*}{p_{intake,in}^*} \quad 2.15$$

In the real case, the balance equations due to the presence of heat exchangers and the fogging system are also introduced.

2.2.1.2 Compressor

We now turn to the characteristic equations of the compressor for which the performance parameters are calculated using the properties of the inlet and outlet gas. Since the compressor has SAS systems, we can write the flow balance equation as follows:

$$\dot{m}_3 = \dot{m}_2 - \dot{m}_{disc} - \sum_i^{Ext} \dot{m}_{E,i} \quad 2.16$$

Where the summation represents the air flow rate extracted by the secondary air systems, and the \dot{m}_{disc} is a component which, in the case of cooling of the compressor outlet section, leads to an increase in the output flow rate. From the heat balance it is possible to derive the power consumed by the compressor:

$$P_{CO} = \dot{m}_{3a} \cdot (h_{3a}^* - h_2^*) + \sum_i^{Ext} \dot{m}_{E,i} \cdot (h_{E,i}^* - h_2^*) \quad 2.17$$

A fundamental parameter for evaluating the compressor's state of the art is the polytropic efficiency. This efficiency has the advantage of not taking into account counter-recovery work, which is not a sign of machine inefficiency. In fact, this is due to friction and dissipation that introduces heat into the gas by expanding it and thus making compression more onerous. The polytropic transformation traces a real transformation of the gas from the conditions at the extremes. The polytropic efficiency is therefore the ratio between the polytropic work and the real work and is defined as follows:

$$\eta_{p,bl,CO} = \frac{R_2 \cdot \ln \frac{p_3^*}{p_2^*}}{s(T_3^*, p_2^*) - s(T_2^*, p_2^*)} \quad 2.18$$

In the same way, polytropic efficiencies are defined by taking into account the properties measured in each secondary air system, allowing polytropic efficiency for different compressor sectors.

$$\eta_{E,i} = \frac{R_2 \cdot \ln \frac{p_{E,i}^*}{p_2^*}}{s(T_{E,i}^*, p_2^*) - s(T_2^*, p_2^*)} \quad 2.19$$

Furthermore, through correlations it is possible to evaluate the total pressure losses at the inlet and outlet of the compressor at the diffuser as a function of a loss coefficient and the evolving flow rate.

The parameters for accessing the maps and obtaining the performance values are listed below, as well as the parameters on which the characteristic maps are defined:

- blading total pressure ratio: $\pi_{CO,bl} = \frac{p_3^*}{p_2^*}$
- Flange total pressure ratio: $\pi_{CO,fl} = \frac{p_{31}^*}{p_1^*}$
- Relative reduced massflow: $\dot{m}_{rel,red,2} = \frac{\dot{m}_2}{\dot{m}_{ref}} \cdot \frac{p_{ref}^*}{p_2^*} \cdot \frac{\sqrt{R_2 \cdot T_2^*}}{\sqrt{R_{ref} \cdot T_{ref}^*}}$
- Relative reduced speed: $n_{rel,red} = \frac{n}{n_{ref}} \cdot \frac{\sqrt{R_2 \cdot T_2^*}}{\sqrt{R_{ref} \cdot T_{ref}^*}}$

Hence, it is possible to interpolate the following parameters from the characteristic map of the component:

- Relative blading polytropic efficiency: $\eta_{rel,p,bl,CO} = f(n_{rel,red}, VIGV, \pi_{rel,bl})$
- Relative reduced mass flow: $\dot{m}_{rel,red} = f(n_{rel,red}, VIGV, \pi_{rel,bl})$
- Relative bleed efficiency: $\eta_{rel,E,i} = f(n_{rel,red}, VIGV, \pi_{rel,bl})$
- Relative bleed pressure: $p_{rel,E,i}^* = f(n_{rel,red}, VIGV, \pi_{rel,bl})$

2.2.1.3 Combustor

The combustor is a delicate component where, due to the high temperatures, little information is available on the thermophysical conditions of the gas, which can be derived from the heat balance shown below.

$$\dot{m}_4 \cdot h_4^* = \dot{m}_{31} \cdot h_{31}^* + (1 - \varepsilon_{loss}) \cdot \eta_{combustion} \cdot \dot{m}_f \cdot (LHV + h_s) \quad 2.20$$

Where the mass balance is given by the following:

$$\dot{m}_4 = \dot{m}_{31} + \dot{m}_f + \dot{m}_w \quad 2.21$$

The combustor is subject to cold losses due to the viscosity of the fluid, so friction, and hot losses since the process is not adiabatic.

$$\Delta p_{CC,rel}^* = \frac{p_{31}^* - p_4^*}{p_{31}^*} = \frac{\Delta p_{friction}^* + \Delta p_{heat}^*}{p_{31}^*} \quad 2.22$$

Where friction losses can be estimated from the classic equation that considers a loss coefficient assessed at the design stage.

$$\Delta p_{friction}^* = \zeta_{friction} \cdot \frac{\dot{m}^2}{\rho_{31}} \quad 2.23$$

While hot losses are derived from the following equation which considers the hot gas temperature and a loss coefficient also estimated by the combustor team.

$$\Delta p_{heat}^* = \zeta_{heat} \cdot \left(\frac{T_4^*}{T_{31}^*} - 1 \right) \cdot \frac{\dot{m}^2}{\rho_{31}} \quad 2.24$$

From the heat introduced into the combustion chamber Q_f it is possible to derive the flame temperature via the balance that considers the flow rate bypassing the primary combustion zone.

$$h_{fl}^* = \frac{(\dot{m}_{31} - \dot{m}_{CC,TCLA}) \cdot h_{31}^* + Q_f}{\dot{m}_{31} - \dot{m}_{CC,TCLA} + \dot{m}_f} \quad 2.25$$

$$T_{fl}^* = f(h_{fl}^*) \quad 2.26$$

2.2.1.4 Turbine

To assess the actual power available to the turbine, it is necessary to subtract the pumping power due to the transport of the air tapped by the compressor inside the turbine and the windage power due to the resistance to rotation caused by the air present between the fixed and rotating parts from the power assessed between the bladed area.

$$P_{shaft,TU} = P_{bl,TU} - P_{pumping} - P_{windage} \quad 2.27$$

These absorbed powers are provided by the SAS team, which allows an estimate to be made.

As with the compressor, the efficiency parameter used for the most is the polytropic efficiency, defined between turbine inlet and outlet to be:

$$\eta_{p,bl,TU} = \frac{s(T_5^*,p_5^*) - s(T_{ISO}^*,p_5^*)}{R_5 \cdot \ln \frac{p_5^*}{p_4^*}} \quad 2.28$$

Which can also be defined for the entire flange meaning that the output section of the diffuser is taken as the output condition.

$$\eta_{p,fl,TU} = \frac{s(T_9^*,p_9^*) - s(T_{ISO}^*,p_9^*)}{R_9 \cdot \ln \frac{p_9^*}{p_4^*}} \quad 2.29$$

The actual temperature at the inlet of the first turbine stator is calculated considering all the air flow entering the combustion chamber.

$$h_4^* = \frac{\dot{m}_{31} \cdot h_{31}^* + Q_f}{\dot{m}_{31} + \dot{m}_f} \quad 2.30$$

$$T_4^* = f(h_4^*) \quad 2.31$$

Taking into account the cooling flow rates that are fed into the turbine, it is possible through the balance to estimate the temperature at the stator outlet (SOT).

$$h_{SOT}^* = \frac{\dot{m}_{31} \cdot h_{31}^* + Q_f + \sum_{i=1}^{N_{CLA,V1}} \dot{m}_i \cdot h_i^*}{\dot{m}_{31} + \dot{m}_f + \sum_{i=1}^{N_{CLA,V1}} \dot{m}_i} \quad 2.32$$

$$T_{SOT}^* = f(h_{SOT}^*) \quad 2.33$$

Finally, we come to the most important temperature, which is calculated by the control system and therefore used as input within the software. This is the turbine inlet mix temperature defined by the ISO 2314 standard, obtained from the hot gas balance with all the cooling flows introduced into the turbine.

$$h_{mix}^* = h_5^* + \frac{\dot{m}_4 \cdot h_4^* + \sum_{i=1}^N \dot{m}_i \cdot h_i^* - \dot{m}_5 \cdot h_5^*}{\dot{m}_5} \quad 2.34$$

$$T_{mix}^* = TIT_{mix} = TIT_{ISO} = f(h_{mix}^*) \quad 2.35$$

As in the case of the compressor, the non-dimensional parameters that are used to access the characteristic maps of the turbine and the parameters on which they are defined are shown:

- blading total pressure ratio: $\pi_{TU,bl}^* = \frac{p_4^*}{p_5^*}$
- Flange total pressure ratio: $\pi_{TU,fl}^* = \frac{p_4^*}{p_9^*}$
- Relative reduced massflow: $\dot{m}_{rel,red} = \frac{\dot{m}_4}{\dot{m}_{ref}} \cdot \frac{p_{ref}^*}{p_4^*} \cdot \frac{\sqrt{\gamma_{ref}}}{\sqrt{\gamma_4}} \frac{\sqrt{R_4 \cdot T_4^*}}{\sqrt{R_{ref} \cdot T_{ref}^*}}$
- Relative reduced speed: $n_{rel,red} = \frac{n}{n_{ref}} \cdot \frac{\sqrt{\gamma_{ref} \cdot R_{ref} \cdot T_{ref}^*}}{\sqrt{\gamma_4 \cdot R_4 \cdot T_4^*}}$

In order to match the diffuser, it is necessary to estimate the flow swirl at the turbine outlet, which is derived as a function of $\dot{m}_{rel,red}$ and $n_{rel,red}$.

2.2.1.5 Diffusor

The diffuser is characterised by its low flow rate and its performance parameters, which include pressure recovery coefficient and total pressure loss. These parameters are defined as follows:

$$\dot{m}_{red,5} = \dot{m}_5 \frac{\sqrt{R_5 \cdot T_5^*}}{p_5^* \cdot A_5} \quad 2.35$$

$$\Delta p_{TU,dif,rel}^* = \frac{p_5^* - p_9}{p_5^*} \quad 2.36$$

$$c_p = \frac{p_9 - p_5}{p_5^* - p_5} \quad 2.37$$

The dynamic head ($p_5^* - p_5$) is calculated by using the mean velocity calculated by the massflow, flow area and density.

Another parameter is also defined which is the diffuser recovery factor which is calculated as a function of the estimated swirl angle at the turbine outlet and is also defined as:

$$\lambda = \frac{h_{9s} - h_5}{h_5^* - h_5} = 1 - \frac{2 \cdot (h_5^* - h_{9s})}{c_5^2} \quad 2.38$$

$$\frac{\lambda}{\lambda_{ref}} = f(\alpha_{in} - \alpha_{in,ref}) \quad 2.39$$

2.2.1.6 Secondary air system

Secondary air systems are modelled as piping characterised by a map showing the reduced flow rate as a function of pressure ratio. The latter is generally defined as the ratio between the pressure evaluated after the orifice or control valve, which manages the flow rate in the turbine cooling systems, and the pressure evaluated at the turbine inlet. This definition may vary depending on which pipeline is being considered.

$$\dot{m}_{red} = \dot{m}_{supply} \cdot \frac{\sqrt{R_{supply} \cdot T_{supply}^*}}{p_{supply}^*} \quad 2.40$$

$$\pi_{supply}^* = \frac{p_{supply}^*}{p_{sink}^*} \quad 2.41$$

2.2.1.7 Exhaust system

The exhaust duct has several components that cause pressure losses. Especially in the case of a combined cycle where there is a recovery boiler. Consequently, losses can be estimated by scaling the losses evaluated under reference conditions. Generally, this loss is measured and used as input in heat balances.

$$\Delta p_{exh} = \Delta p_{exh,ref} \cdot \frac{\dot{m}_{exh}^2}{\dot{m}_{exh,ref}^2} \cdot \frac{T_{exh}^*}{T_{exh,ref}^*} \cdot \frac{p_{amb,ref}}{p_{amb}} \quad 2.43$$

Due to the high complexity of the system, the main parameters and fundamental equations of its most significant components were given in order to provide an idea of the modelling. In addition to the balance equations and calculated parameters, the model also includes geometric information, such as the inlet and outlet sections of the components, which allow the flow velocities within them to be determined and, consequently, the previously mentioned parameters. As regards the estimation of the power generated by the combined cycle, which is not of primary importance in the objectives of these calculations, we proceed by estimating the efficiency of the steam cycle as a function of the exhaust gas temperature.

In summary, the heat balance is based on energy conservation equations and mass conservation equations. By taking advantage of some of the measurements made on the gas turbine, the characteristics of the components implemented in the libraries and the assumptions on mechanical and heat losses, it is possible to carry out calculations that make it possible to obtain information on non-measurable quantities such as the temperature of the gases leaving the combustor, the suction flow rate, the distribution of power in the various components and the efficiencies of the components. The type of calculation is managed by the user, who decides which measurements to trust the most; in fact, there are different types of calculation settings that can also be used to validate each other's calculations. These settings are shown in Figure 2.3 within which the matching schemes are defined. Each of them makes different assumptions; in the results which will be reported in the following chapter, matching scheme 2 has been used, which assumes as reliable the measurement of the fuel flow rate and the turbine exhaust temperature, and consequently derives the compressor inlet flow rate and the turbine swalling capacity, which is the reduced flow rate evaluated at the first turbine stator.

Method \ Parameter	Heat Input	Compressor mred	Turbine mred	Exhaust temperature	CO2	O2
MS1	output	Input	output	Input	output	output
MS2	Input	output	output	Input	output	output
MS3	Input	Input	output	output	output	output
MS4	Input	output	Input	output	output	output
MS7	output	output	Input	Input	output	output
MS8	Input	output	output	output	Input	output
MS9	Input	output	output	output	output	Input

Figure 2.3 - Matching scheme table

In addition to these inputs in the heat balances, the measures given in the first paragraphs of the chapter are used:

- *Ambient condition*: ambient temperature, humidity and pressure;
- *Operating condition*: power, VIGV position, rotational speed, generator power factor;
- *Fuel measurment*: composition, injection temperature, massflow;
- *SAS measurement*: temperature, pressure and massflow after the orifice/control valve;
- *Pressure losses*: inlet pressure losses, exhaust pressure losses;
- *Gross Power*;

Given the large number of measurements that are used in the calculations, it is easy to see how these calculations can be affected by incorrect measurements but also by simple measurement uncertainty. To assess the effects of measurement uncertainty, there is a possible calculation called *Probabilistic Heat Balance* that takes this into account. In heat balances, the software is asked to use measurements and calibrate the GT model parameters to validate the measurements used as input. In the probabilistic mode, measurements with the associated uncertainty are used as input and the model parameters are then calibrated to validate the measurements but propagate the uncertainty information. This mode certainly requires a higher calculation cost and therefore longer calculation times.

2.2.2 - Synthesis

Synthesis are calculations that provide an estimate of how the gas turbine should perform according to the characteristics of the components using only the fundamental information of the operating condition as input for the software. In fact, to perform *synthesis* calculations, the following are set as input:

- *Pressure losses*: inlet pressure losses, exhaust pressure losses.
- *VIGV position*.
- *Ambient condition*: ambient temperature, humidity and pressure.
- *Fuel composition*.
- *TIT ISO*.

In addition to these measurements, parameters such as component cross-sections, pressure drop coefficients in the pipes, and those parameters that provide the variables that were used as inputs in the case of *heat balances* are fixed. In substance, this is a calculation that relies more on the quality of the model and thus on the characteristic maps built. In order to have good *synthesis* results, it is important that the model is as representative as possible of the state of the gas turbine, which is updated periodically, especially when hardware modifications or repairs are introduced. This allows us to have an estimate of how the gas turbine should perform in the period following the construction or updating of the model, making it possible to compare with *heat balances* that are more closely related to the current state of the engine. In addition to allowing us to make a comparison for the balances, they were used to carry out a quality check on the measurements to exclude measurements that are completely wrong.

2.2.3 Ansyn factor

The term *ansyn* is short for analysis by synthesis. These factors are automatically calculated when launching the heat balance. They describe the distance between the synthesis calculations and the heat balances, hence the deviation between the model and the validation results. They therefore allow, when analysed over time, the presence of GT degradation to be noted; in fact, they will be used as results in the next chapters to show how monitoring is carried out.

These factors are defined for various components such as the compressor, turbine, secondary air, diffuser and combustor systems. They are generally multiplicative factors for mass flow rates and additive factors for efficiencies and pressure levels. Thus, they represent the

deviation between results obtained from balances and results obtained through component characteristics. Examples of definitions are given below.

In the case of reduced mass flow rates in secondary system pipelines, the Ansyn factor is defined as follows:

$$ANSYN \text{ reduced massflow} = \frac{\text{reduced massflow measured}}{\text{reduced massflow predicted}}$$

Where the reduced flow rate at the numerator is calculated by heat balances that rely on the measurement of the mass flow rate within the pipe and the flow rate at the denominator by synthesis calculations.

While in the case of efficiency, there is a deviation in percentage terms between the value calculated in heat balance and synthesis.

$$ANSYN \text{ efficiency} = \eta_{HB} - \eta_{SYN}$$

It is intuitable that these factors are dependent on the quality of the model, which very often depends on the operating condition and therefore primarily on the VIGV position. It is indeed possible that the model has a better fit to the actual condition when the gas turbine performs at base load, consequently the deviation from the target value will be greater in conditions where the model less represents reality. It is therefore important that however different this may be from the target value, 0 or 1 depending on the definition, it remains constant over time at fixed VIGV, otherwise there is the symptom of degradation

2.3 – Solver

To solve the system of equations, the software uses the Block Oriented Process solver, which is an optimisation algorithm that minimises the deviation between measured quantities and the corresponding model variables. The BOP allows the system of non-linear equations to be solved using the Newton Rhapsion method to achieve convergence and thus calibration between measurements and model.

As the name suggests, this algorithm organises equations into functional blocks according to their functionality and dependency. This organisation simplifies the process of solving the system, allowing each block to be treated separately or in parallel. This type of approach can be particularly useful when there are complex dependencies or interactions between the variables in the system, making it difficult to solve the system of non-linear equations

directly. By dividing the system into functional blocks, it is possible to apply specific solving techniques to each block and then combine the solutions to obtain an overall solution.

The Newton Rhapsion method is an iterative numerical technique used in engineering to find the zero of a function. In our case, this is an error function. To obtain this result, the method starts with an initial assumed value x_0 , the value of the function at that point $f(x_0)$ and its derivative $f'(x_0)$. From that point, the x-axis is intercepted to obtain the next new point using the following formula.

$$x_{n+1} = x_n - \frac{f(x_n)}{f'(x_n)}$$

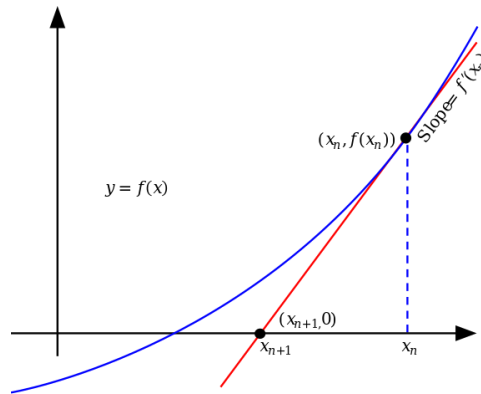


Figure 2.3 - Newton Rhapsion method

Consequently, one proceeds iteratively until zero is found, or in the case of complex functions $f(x_{n+1}) < \epsilon$, where the latter is a tolerance that in Alpeg is fixed at 10^{-4} .

It is easy to see the weakness of this algorithm lies in the derivative, which in the case of non-continuous functions is difficult to obtain. There may be many other causes, such as if the solution is not physically possible, for example the efficiency of a turbine stage turns out to be negative. Another way if the specific calculation falls outside the definition of the characteristic of the component, or even the chance that an equation has a null value as denominator.

The advantage of this method is that every variable can be either set to a fix value or to be set free without changing the iteration strategy.

To improve the speed at which the algorithm reaches convergence, it is important that the first guess is chosen and that the model is not overly complex. In fact, greater complexity leads to convergence problems, thus preferring fewer equations with less redundancy of similar parameters.

3. Automated Heat Balances

In this chapter, we will explore the process of automating and improving the quality of heat balances develop within this thesis work. We will discuss measurement taking criteria, data pre-processing and the results obtained, highlighting how these can reveal degradation. Figure 3.1 shows a flow chart illustrating the steps required to obtain high-quality heat balances. In the following paragraphs, we will examine each section in detail.

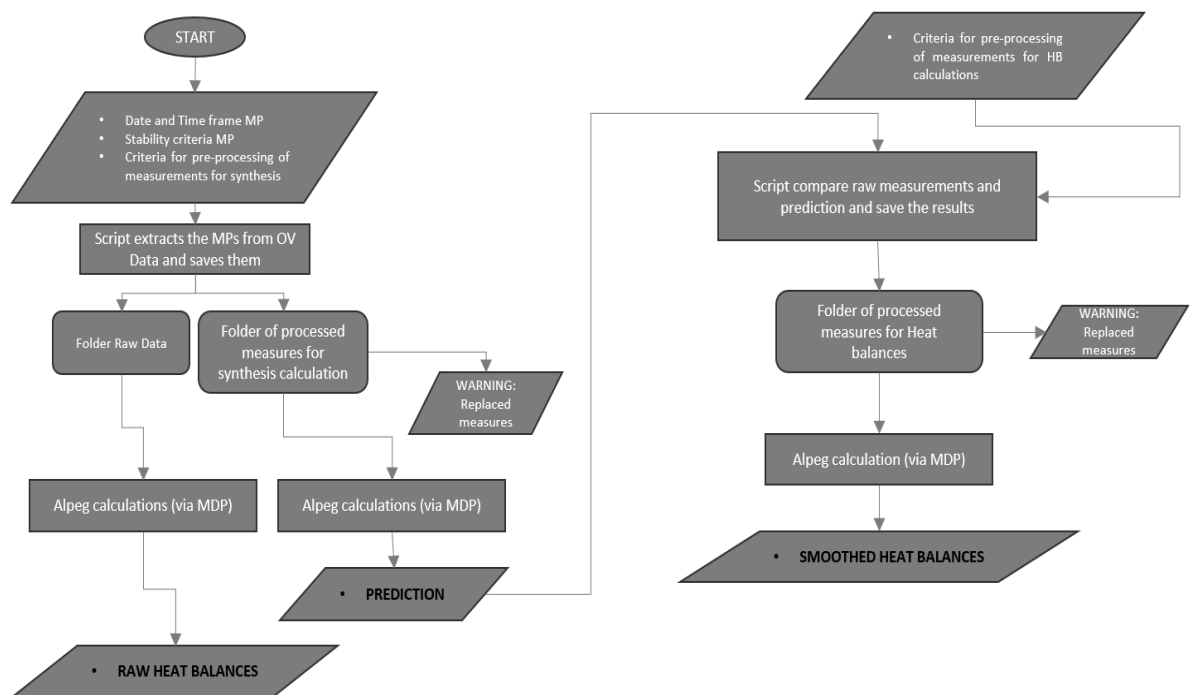


Figure 3.1 - Automated Heat Balances Flowchart

3.1 – Description

The aim of the thesis is to ensure frequent monitoring of the GT in an automated manner to detect any malfunctions, failures or degradations that may affect the performance of the machine while maintaining the reliability of the performance test calculations. During performance tests, well-defined sampling criteria are followed to obtain reliable measurements and performance calculations that reflect the actual state of the engine. Consequently, it was necessary to develop a system that guarantees reliable measurements, sampled according to criteria that stabilize the measurement point. These criteria can then be improved over time through experience. In this discussion, we will define measurement point (MP) as any set of measurements taken at a given point in time.

The initial phase of the thesis involved the development of a system to automate the sampling of measurement points. This implementation was realized using an Excel file, within which was incorporated an add-in capable of communicating with a dedicated database for each engine. The database stores a vast amount of data via communication with the gas turbine (GT) control system. To mitigate significant fluctuations in the raw measurements transmitted by the sensors, time-averaged data can be downloaded via the Excel spreadsheet at a user-defined time interval.

To make this process dynamic, macros have been implemented within the sheet, managed by an external script. Through a user interface (Figure 3.2), it is possible to define the date and time of the start and end of sampling, the distance between each measurement point and the duration of the measurement point, from which the averaged value of each measurement within the measurement point (MP) will then be taken. Dynamically, for each indicated day, the script subdivides the assigned time range according to the distance of each MP, generating a text file containing the measurements, which will be used to perform heat balances.

INPUT		UNIT
Start date	2024/02/26	yyyy/mm/dd
End date	2024/02/26	yyyy/mm/dd
Duration MP	1	min
Distance between MP	9	min
Start time MP	18:00	hh:mm
End time MP	19:00	hh:mm

Figure 3.2 – Excel user interface data/time frame

Through the database, it is possible to download information for each measurement within the MP, such as the average value, the minimum value, the maximum value, and the associated maximum deviation. This information is crucial to define a stabilization criterion for the MP. In fact, for the sampling and saving of the MP to be successfully completed, certain criteria must be fulfilled.

The need to define a stabilization criterion derives from the influence of thermal transients within the gas turbine (GT), during which significant variations in performance may occur due to temporary changes in the engine's physical structure.

These thermal transients can result in measurements and calculations that do not reflect the actual state of the machine. During thermal transients within a gas turbine, changes in the thermal state can occur resulting in a change in component geometry and the heat flow into the parts (e.g. into the rotor) that changes the performance. In fact, thermal expansion of the blades and stator case can temporarily affect the distances between the rotating and static parts, changing the efficiency of the compressor and turbine. For example, during a cold

start, the blades may expand faster than the stator case, leading to the temporary closure of the tip gap of the blades and increasing the transformation efficiency.

In addition, sensors may experience frequency response problems during highly unstable conditions, which can lead to incorrect measurements. Therefore, it is crucial to stabilize measurements during these thermal transients to obtain accurate assessments of GT performance and associated calculations.

To mitigate the effects of engine instability, criteria have been defined that can be improved and refined with experience. These are based on verifying that the MP is in a stable condition by checking the variations in the power and position of the VIGV over time, both at the point of measurement itself and in the minutes before the MP. The control scheme is shown in the figure. The check is based on the average value of the MP. It is therefore checked that in the minutes before it, the minimum and maximum values do not exceed a certain user-defined threshold value. In the same way, a check is made in the duration on the MP. Figure 3.3 shows the criteria, while Figure 3.4 shows the corresponding Excel sheet interface for setting tolerances. In this way, a limited number of MP are obtained.

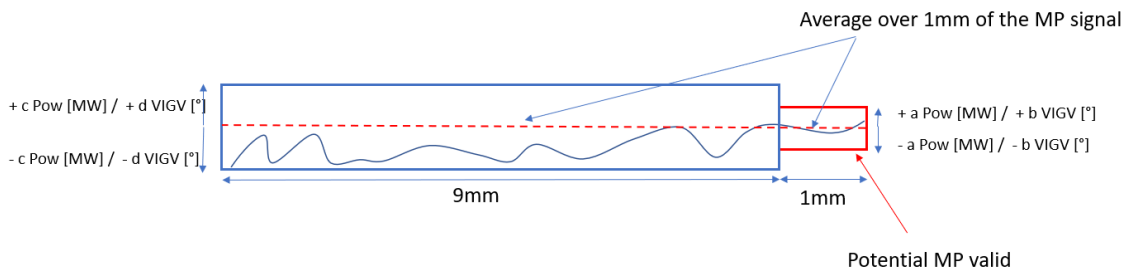


Figure 3.3 - Stabilization criteria MP

	CONTROL	PARAMETER	DEVIATION [+/-]
c	Before MP	Power [MW]	8
d	Before MP	VIGV [°]	1.5
a	MP	Power [MW]	4
b	MP	VIGV [°]	0.75

Figure 3.4 - User interface to set stabilization tolerances

Once the stabilization criteria had been established, a second phase was started, which involved the generation of reference values to check the measurements. The existing MDP pre-processing system, which also facilitates the automatic launch of heat balances in *Alpeg*, is not able to directly compare measurements with reference values. Rather, MDP identifies erroneous measurements within the redundant data and generates values +/- to be assigned to

the corresponding variables within *Alpeg*. To address this limitation, it was decided to perform *synthesis* calculations to obtain reference values, which will then be compared with the raw measurements during the input processing phase for heat balances.

During the introduction to heat balances, several measurement problems were identified. These problems also affected the measurements used to carry out the synthesis calculations. To obtain reliable reference values to compare with the measurements, it was therefore necessary to process two measurements in particular: the pressure drop in the intake duct and the pressure drop at the exhaust. Problems have been noticed in the past with these measurements, which cause an incorrect evaluation of the mass flow rate and an incorrect evaluation of the turbine efficiency, respectively, as will be shown in the results.

Since the exhaust pressure drop is evaluated a posteriori as the difference between the pressure evaluated at the turbine exhaust and the ambient pressure, in the event of incorrect evaluation of the exhaust pressure, the exhaust pressure drop may turn out to be negative, resulting in completely faulty calculations. To overcome this problem, a pre-processing of these two measurements was implemented in the script to obtain reliable predictions. To do this, the component characteristic was introduced into the script in order to obtain a reference value to verify the raw measurements, without going through the *Alpeg* software. Therefore, the characteristics were defined through a linear interpolation to obtain the prediction values, which are defined as follows:

- *Inlet pressure drop*: as function of T_{amb} and VIGV as it is dependent on the rate of flow. The effect of pressure is taken into account through the definition of the setpoint value which is assigned by the user. This is defined for ISO condition (VIGV = 0°) and represents the value from which the reference value corresponding to the actual operating condition is then interpolated.
- *Exhaust pressure drop*: as function of T_{amb} and VIGV. In the same way as the inlet losses, the effect of pressure in the setpoint value for ISO condition and VIGV = 0° has to be taken into account. From this value, the actual reference value of the pressure at the exhaust can be calculated by adding it to the ambient pressure. Once the exhaust pressure reference value has been obtained, it is possible to verify that the measurement is inside the user-defined tolerance to the reference value.

In the interface, the user also defines the tolerance within which the measurement must comply with the reference value. In addition to these measurements, an ambient pressure check is also performed. As ambient pressure is difficult to predict exactly, only a fixed reference value and a tolerance on it can be defined.

PREPROCESSING PREDICTION INPUT				
PARAMETER	REFERENCE VALUE	UNIT	TOLLERANCE +/-	UNIT
Ambient pressure	1013	mbar	50	mbar
Inlet pressure drop ISO condition	11.4	mbar	6	mbar
Exhaust stati pressure loss ISO cond	38.05	mbar	5	mbar

Figure 3.4 - User interface to define preprocessing criteria for synthesis input measurements

Once this information has been set, it is then possible to launch the script via the python file *launch_marg.py*, which communicates with the Excel file *Marghera_Macro.xlsm*. Once started, it will automatically generate a folder for each day between the specified dates, within which there are subfolders. As can be seen from Figure 3.5, there are the three tags RHB-input, PHB-input and SHB-input. These respectively represent the files containing the raw measurements, the pre-processed measurements for making predictions and finally the pre-processed measurements for making heat balances (smoothed input). The latter remains empty until the prediction calculations are made and the second script *Preproc-SHBinput.py* is run. For each of these, the folder is also created which will contain the corresponding results of the calculations performed afterwards (output folder). The PHB-input and RHB-input folders will contain text files containing the corresponding measurements. In the case of PHB, there will be a sub-folder within which there is a text file containing information on the pre-processing carried out on the inputs used in the synthesis calculations.

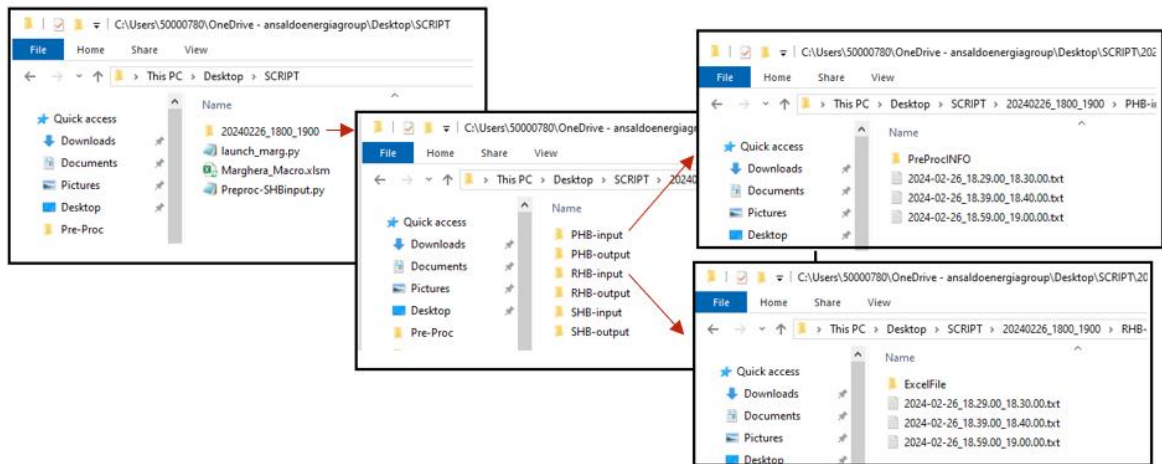


Figure 3.5 Results of the first script

An example of the pre-processing of measurements on which synthesis calculations are performed is presented below. Figure 3.6 shows the file indicating which measurements have been replaced. As can be seen, the exhaust pressure measurement has been replaced. Since the exhaust pressure measurement is redundant, it is possible to check in the measurement list which values the other measurements have. As can be seen, the replacement value is very similar to the value of the other measurements for the same MP.

Processing report			List of measurement	
INFO MP 2023-09-01_19.29.00_19.30.00				
Measurement	Raw value	Corrected value		
MBA30CP001_XQ01	1.01675806596877	1.05096364335163	←	MBA30CP001_XQ01 1.050964
				MBA30CP002_XQ01 1.050734
				MBA30CP003_XQ01 1.049658
				...

Figure 3.6 – Validation of PHB-input preprocessing with other measurements

When reliable measurements have been obtained on which prediction calculations can be made, it is possible to launch the simulations through the MDP tool, to which it is possible to communicate from which directory to read the inputs and in which directory to save the results by using a text file. The software automatically reads all the files in the input folders and creates a file for each of them that can be read by the Alpeg performance tool, which must be opened in the background. Once the calculations are complete, it saves the results in the predefined folder.

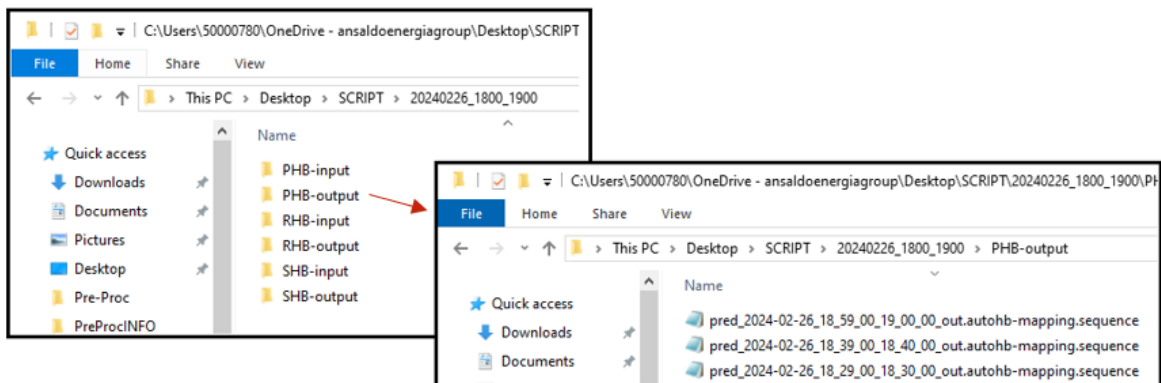


Figure 3.7 Alpeg simulation results

After the predictions have been obtained, we move on to the last step, which involves checking the quality of the raw measurements. The appropriate script, *Preproc-SHBinput.py*, allows the results of the prediction calculations saved in the corresponding folder to be read automatically, together with the corresponding raw measurements. For each measurement point (MP), the script compares the predicted values with the raw measurements.

The user has the possibility of defining, via the interface available on the Excel sheet, the tolerances to be applied according to the reliability of the measurements he wants to pre-process. These tolerances can be defined as an absolute value or as a percentage value in

relation to the reference value calculated during synthesis. Control is performed on each raw measurement individually, including the treatment of redundant measurements one at a time. Figure 3.8 shows the user interface available on the Excel sheet for defining tolerances.

PREPROCESSING HEAT BALANCES INPUT				
ALPEG TAGNAME	DESCRIPTION	LOWER TOL	UPPER TOLL	abs / %
TURBDIF.GASOUT.TT	TAT	100	100	abs
GENO.PGROSS	GT Gross Power	100	100	%
GLOBAL.FBFUEL M	Actual fuel mass flow for FB	100	100	%
GLOBAL.SBFUEL M	Actual fuel mass flow for SB	100	100	%
PL10.TT IN	MBH10 avg total temperature	20	20	abs
PL10.PT IN	MBH10 total pressure plenum	5	5	%
PL20.TT IN	MBH20 avg total temperature	20	20	abs
PL20.PT IN	MBH20 total pressure plenum	5	5	%
COMBPLE.PT IN	Total pressure (pk2)	5	5	%
COMBPLE.TT IN	Total temperature (Tk2)	15	15	abs
MBH30REF.PT IN	Total pressure (used in calcul	100	100	%
MBH20REF.PT IN	Total pressure (used in calcul	100	100	%
MBH10REF.PT IN	Total pressure (used in calcul	100	100	%
TSTRUTS.COOL.GASIN.M	MBH55 massflow from ambie	50	50	%
GLOBAL.MBH10CF001 MEAS	MBH10 measured flow	5	10	%
GLOBAL.MBH20 TOTAL MEAS	MBH20 measured flow	5	5	%
GLOBAL.MBH30 STATOR M	MBH30 Turbine Stator	100	100	%
GLOBAL.MBH30 ROTOR M	MBH30 Turbine Rotor	5	5	%
GLOBAL.MBH30CF100 MEAS	MBH30 measured flow	5	5	%

Figure 3.8 - User interface for setting HBs pre-processing criteria

After defining the tolerances and running the python script, the text files for each MP containing the preprocessed measurements will be available in the SHB-input folder. In addition, a text file containing a report of the measurements replaced during preprocessing will be available in a subfolder.

Through this pre-processing process, it was possible to identify several problems in the measurements. As shown in the table in the figure above, the most problematic measurements concern the flow rates of secondary air systems (SAS). The flow measurement based on a pressure measurement connected via a pressure measurement sensing line with the sensor itself. Due to condensation within the measurement sensing line the measurement can be disturbed resulting in a wrong flow measurement. Before any proper measurement it is required to purge these lines. An example of this is shown below, where pipe cleaning is performed and a significant change in the measurement of the total flow rate within the MBH30 pipe (MBH30CF020) is observed, which is 5 kg/s. It is noticeable that cleaning the pipe that carries the flow to cool the rotor also results in a slight change in the flow rate, which is approximately 2 kg/s (MBH30CF060).

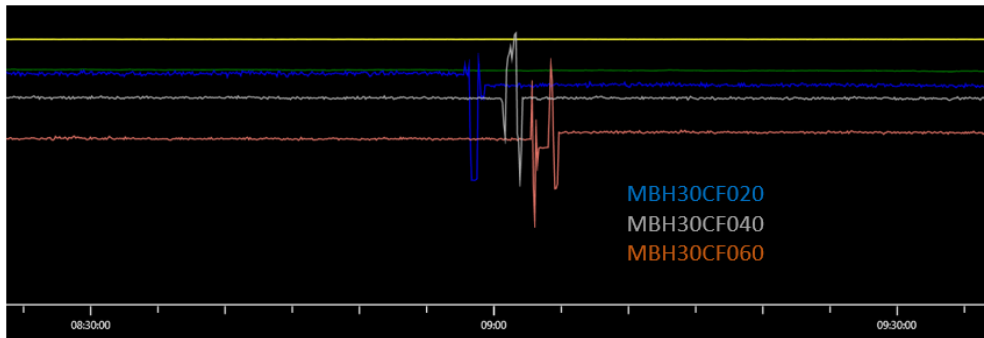


Figure 3.9 - Ov Data raw measurement view available on the OvData viewer

The pre-processing system detects and corrects the error in the flow measurement before purging the pipes, as shown in the figure 3.10. By identifying the anomaly in the measurement before purging, the algorithm makes a correction to the value, thus improving the overall reliability of the results. As can be seen, once the purging was carried out, the total mass flow was no longer replaced.

MP: 2023-06-06_08_19_00_08_20_00	RAW VALUE	SMOOTHED VALUE
MBH30CF020_CALC	8.901308	3.119257
MP: 2023-06-06_08_29_00_08_30_00	RAW VALUE	SMOOTHED VALUE
MBH30CF020_CALC	9.010482	3.181751
MP: 2023-06-06_08_39_00_08_40_00	RAW VALUE	SMOOTHED VALUE
MBH30CF020_CALC	8.905374	3.058825
MP: 2023-06-06_08_49_00_08_50_00	RAW VALUE	SMOOTHED VALUE
MBH30CF020_CALC	8.966242	2.974458
MP: 2023-06-06_09_19_00_09_20_00	RAW VALUE	SMOOTHED VALUE
MBH20CF040_CALC	4.474028	1.557962
MBH20CP040_XQ01	1.985773	1.162740
MP: 2023-06-06_09_29_00_09_30_00	RAW VALUE	SMOOTHED VALUE

Figure 3.10 SHB input preprocessing report

From the above figure, for the MP obtained at 9:19 a.m., there is a correction to the flow rate at pipe MBH20 (MBH20CF040), as the sampling took place at the exact time when the pipe was purged as shown in the following figure 3.11. Furthermore, the pressure measurement at pipe MBH20 (MBH20CP040) is also replaced, as it too is affected by the purging.

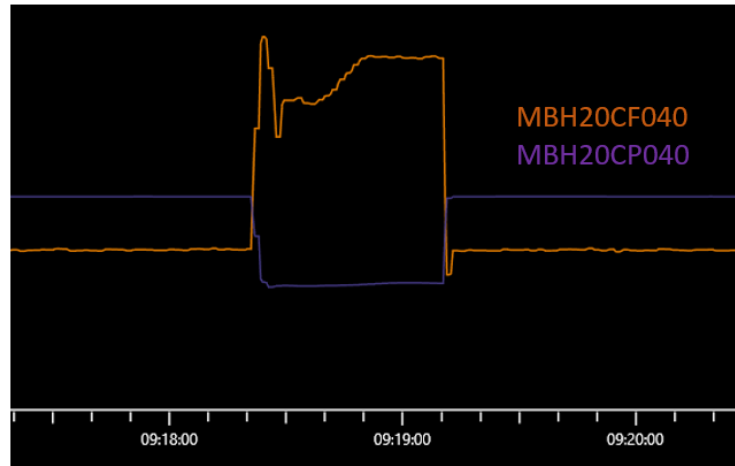


Figure 3.12 Effect of purging on mass flow and pressure measurement of MBH20 pipe

From the above examples, the potential of such a filter can be discerned, however, it is important that the model correctly predicts the measurement if measurement errors are present; therefore, the quality of the model is of importance. These values were validated by comparing the predicted value and the value immediately after purging and a good match was found. In addition to being able to identify erroneous measurements for condensation, it is also able to avoid the peaks of the natural fluctuations of the raw measurements transmitted by the sensor, which, as can be seen in the figure 3.13, can be significant and cause measurement variation of around 4 kg/s affecting the average value obtained in the MP duration.

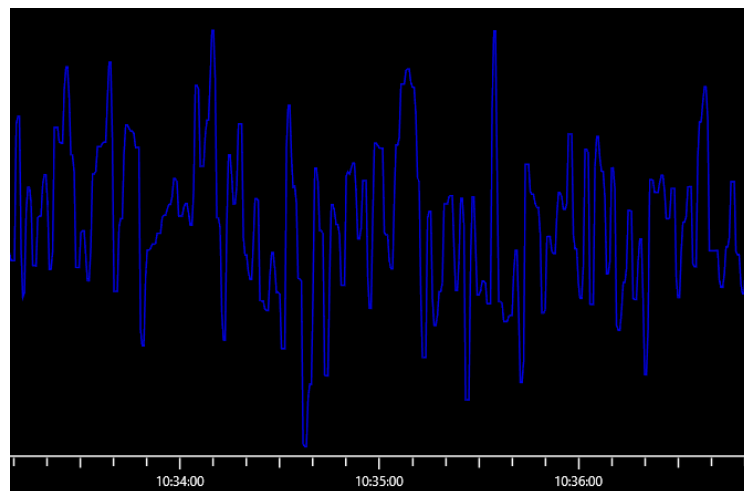


Figure 3.13 Fluctuation of raw measurement against time

In addition, the algorithm identifies completely incorrect measurements due to a broken sensor, as highlighted in the figure below showing a broken thermocouple (MBH10CT011).

This not only allows the measurements to be corrected, but also provides an assessment of the general state of the sensors on the gas turbine.

MP: 2024-02-19_08_39_00_08_40_00		
	RAW VALUE	SMOOTHED VALUE
MBH10CF010_CALC	914080	144663
MBH10CT011_XQ01	-0.124996	0.743039
MP: 2024-02-19_08_59_00_09_00_00		
	RAW VALUE	SMOOTHED VALUE
MBH10CF010_CALC	764485	050081
MBH10CT011_XQ01	-0.124996	0.158898

Figure 3.14 - Pre-processing report show failed sensor

Once the pre-processed measurements have been obtained, heat balances can finally be performed automatically using the MDP instrument again. In the following section, the results will be presented, and a comparison will be made between heat balances based on RHB raw measurements and those based on SHB pre-processed measurements.

3.2 – Results

In this part of the document, the results of heat balances for two plants with GT36 are presented. These results were obtained over several days from the performance test conducted last June. The pre-processing actions were previously examined and validated, and we now proceed to verify the effect of pre-processing on the results of the heat balances.

In order to examine the effects of incorrect measurements, the following section will refer to the previously mentioned examples of measurement problems. To conduct the analysis, Ansyn factors will be used to assess the discrepancy between the validation data (HB) and the predictions of the GT model, as explained above. These factors are used to detect any variations over time, which, if present, could indicate degradation or in the worst case loss of components within the gas turbine.

The following graphs present the results for RHB and SHB using different markers, represented in the legend. A colour differentiation was adopted to check the possible effect of temperature on the results. However, it is expected that there are no significant differences as the model is able to adapt to ambient temperature. It is important to note that the results presented correspond to the base load condition and that the position of the VIGV is between -5 and 5. Initially, we will focus on a temporal overview of the results and then elaborate on the differences between RHB and SHB.

The usefulness of these calculations is therefore demonstrated by showing the degradation in the compressor and turbine over the course of nine months. Figure 3.15 shows the first example of the compressor's Ansyn factor trend over time. This factor is defined as the difference between the calculated polytropic efficiency and that predicted by the model. Considering the first day represented, corresponding to 6 June 2023, it is observed that the GT has a higher efficiency than predicted by the model. This may indicate that the model is not aligned with the state of the GT; however, it is used as a reference point. Looking at the other days, it can be seen that the polytropic efficiency tends to decrease over time, probably due to the accumulation of dirt (fouling), but further investigation could also reveal other potential failures. As shown in the graph in Figure 3.16, the reduced mass flow rate of the compressor decreases over time, in line with its degradation.

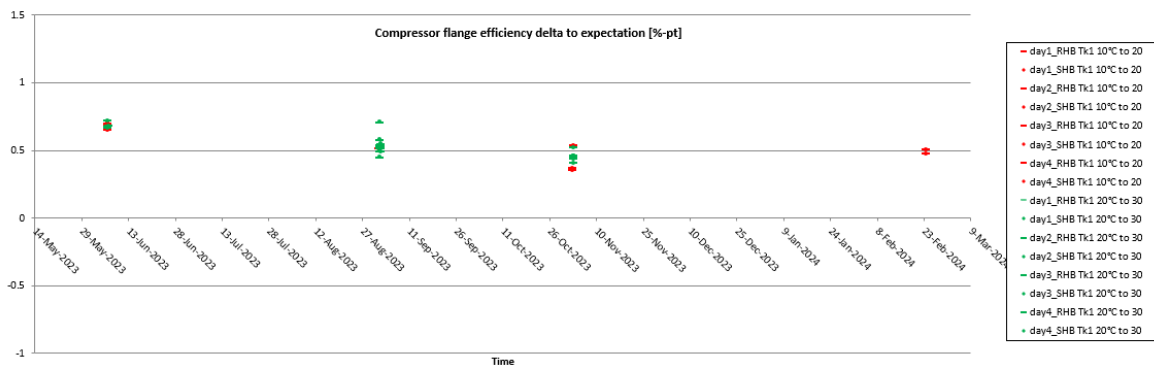


Figure 3.15 Compressor flange efficiency delta to expectation [%] against time show degradation

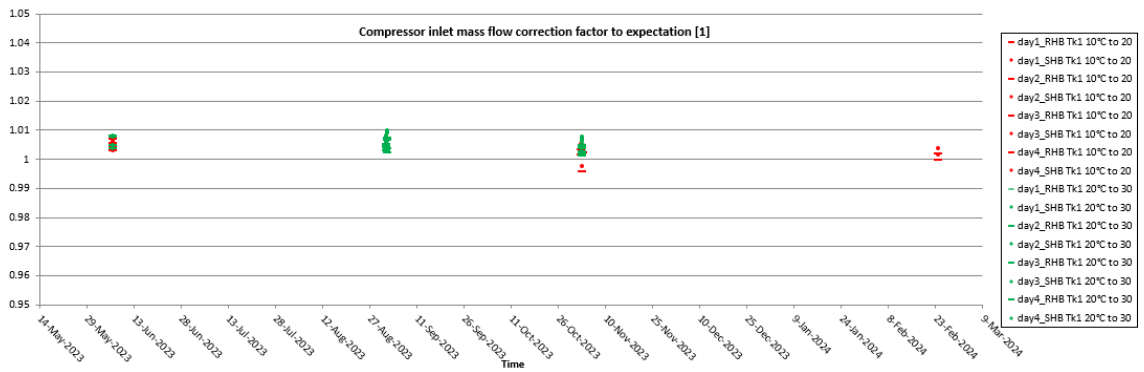


Figure 3.16 Compressor inlet mass flow correction to expectation show descreasing

Figure 3.17 shows the trend of the turbine flange efficiency Ansyn factor, also defined as delta to expectation. Similarly, to what has been observed for the compressor, taking as reference the results of the first day which show a higher efficiency than predicted by the model, a reduction in the turbine efficiency over time can be seen, which could be related to the increase in the tip clearance of the turbine blades.

Figure 3.18 shows the turbine capacity trend, which is used in monitoring to identify possible problems within the turbine. As it is proportional to the passage area, any significant variations would signal significant damage within the turbine. The discrepancy observed between RHBs and SHBs will be explained next.

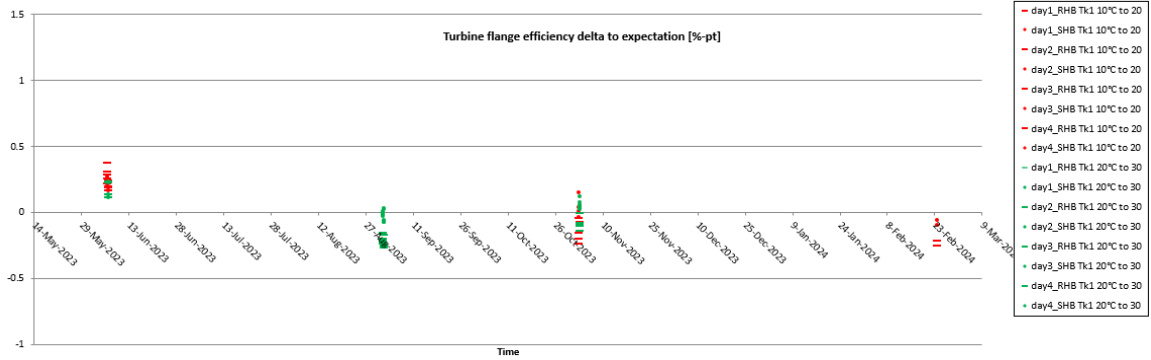


Figure 3.15 Turbine flange efficiency delta to expectation [%] against time show degradation

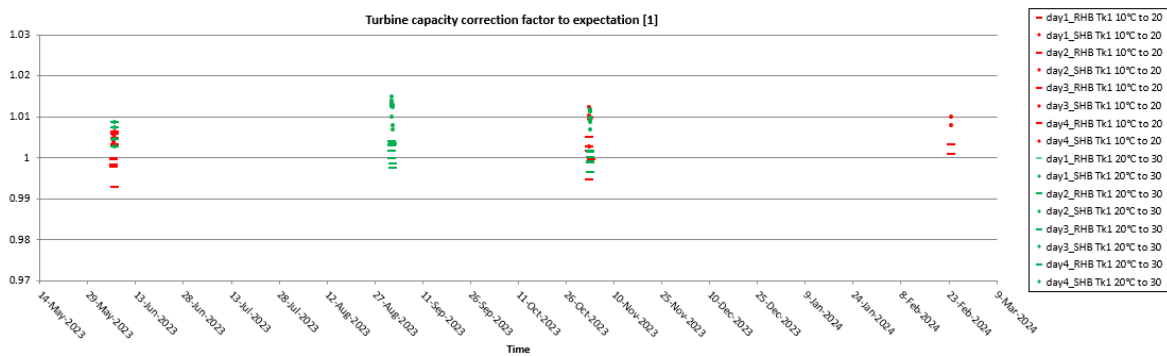


Figure 3.18 Turbine capacity correction to expectations

Beyond the previously mentioned factors, there are those concerning secondary air systems, which provide crucial information on the reduced flow rate within each pipe. These factors are defined as the ratio between the measured reduced flow rate and that predicted by the model. They represent a significant aspect of monitoring as they allow the state of the seals inside the turbine to be assessed.

Since secondary air systems consist of piping with an orifice or control valve inside, it is essential that they provide the correct cooling flow rate to the turbine cooling system. An increase in the flow rate within such piping could indicate an increase in the cross-sectional area, thus suggesting the possible failure of a seal or, in the worst case, the failure of a blade.

In Figure 3.19, there is a slight increase in the flow rate of about 4% between September and October in the MBH10 pipe. As has been shown previously, such measurements are very often incorrect due to the presence of condensation inside the sensor pipe, so the

measurement may be wrong. As shown in Figure 3.8, a maximum permissible deviation of the flow measurement for pipe MBH10 of 10% was set. Therefore, since the deviation of the measured flow rate from the model predicted flow rate is 7%, below the maximum allowed limit, no action is triggered by the preprocessing system. In difference to the other flow rates of the secondary air systems, a larger upper tolerance was imposed as the model underestimates the actual value of the flow rate.

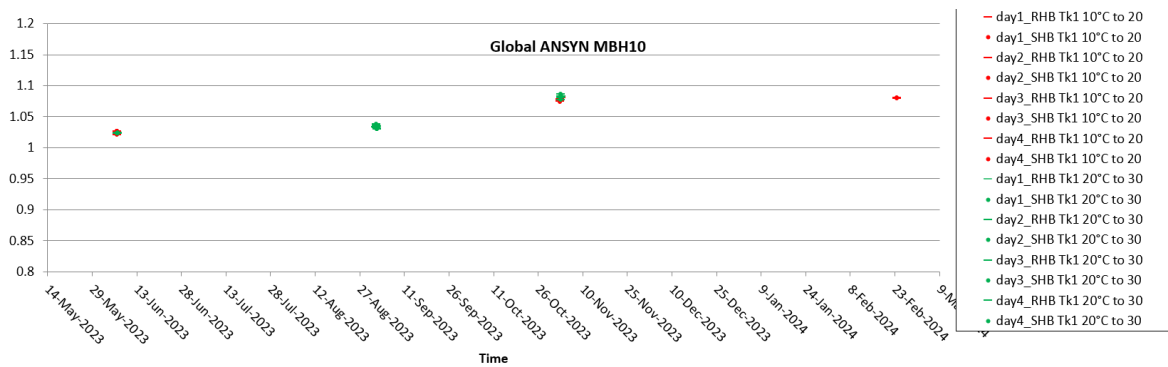


Figure 3.19 SAS MBH10 system ansyn factor

As shown above there is for one specific day a fluctuation in the flow measurement due to the purging of the pipe containing the sensor. As this fluctuation is greater than 5%, the effect of the preprocessing script can be seen. Which corrects in the case of the SHBs, indicated by the dot, the flow rate value with the prediction value calculated in the synthesis calculation. This corresponds to an ansyn factor of approximately one unit. Figure 3.20 shows that the raw flow rate value in the RHB, which comes to be almost 30% above the expected value.

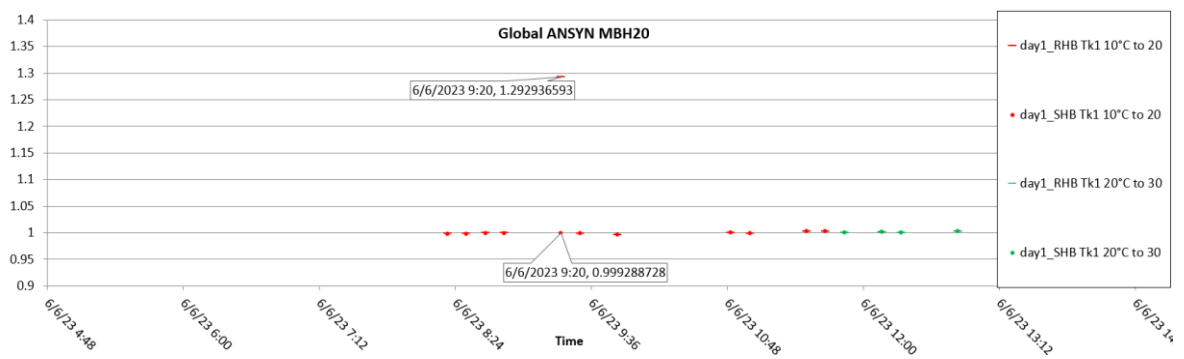


Figure 3.20 MBH20 system ansyn factor

Similarly, it was shown that before the MBH30 pipe was purged, the flow measurement was completely wrong due to condensation close to the sensor, see figure 3.9. In this case, as the flow rates can exceeded one hundred kilograms per second, a tolerance of 2% was imposed. It can therefore be seen in figure 3.21 that at the points prior to purging there is a correction to the flow rate, leading to a unit ansyn. However, at the points following the purge, there is

a measured flow rate 10% higher than the model prediction. This indicates that the model tends to underestimate the actual value of the flow rate. Therefore, it would be necessary to update the model to account for this deviation.

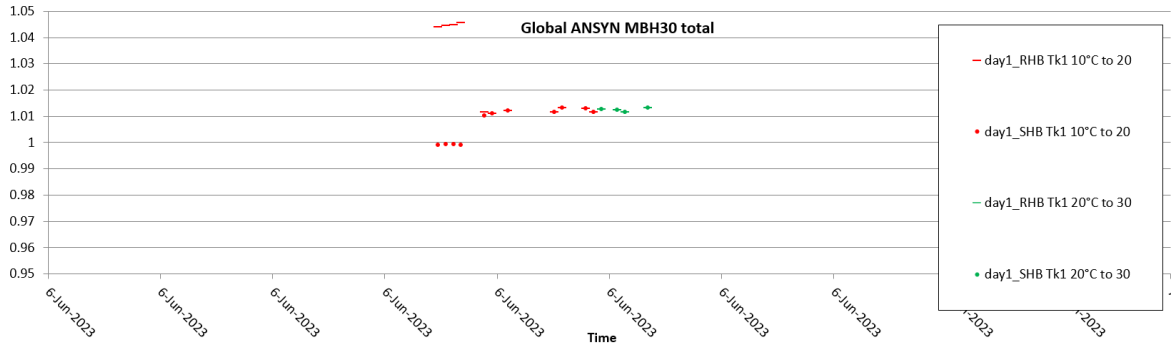


Figure 3.21 MBH30 system ansyn factor

The point after the corrections there is a slight deviation between RHB and SHB, this point is the one that corresponds to the correction of the MBH20 flow measurement. To identify the reasons, it would be necessary to conduct an in-depth analysis, which, however, is not the purpose of this work.

Figure 3.22 shows the Ansyn factor of the turbine capacity, defined as the ratio between the actual and predicted value. It is evident that errors in the measurement of the flow rate led to an incorrect assessment of the turbine capacity, thus affecting the polytropic efficiency of the turbine. Which ansyn factor is defined as the delta with respect to expectation and is shown in Figure 3.23.

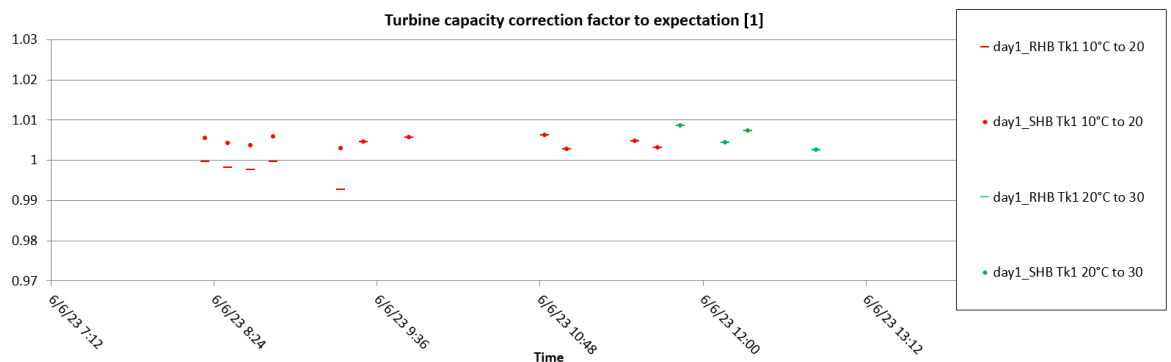


Figure 3.22 Turbine capacity ansyn factor

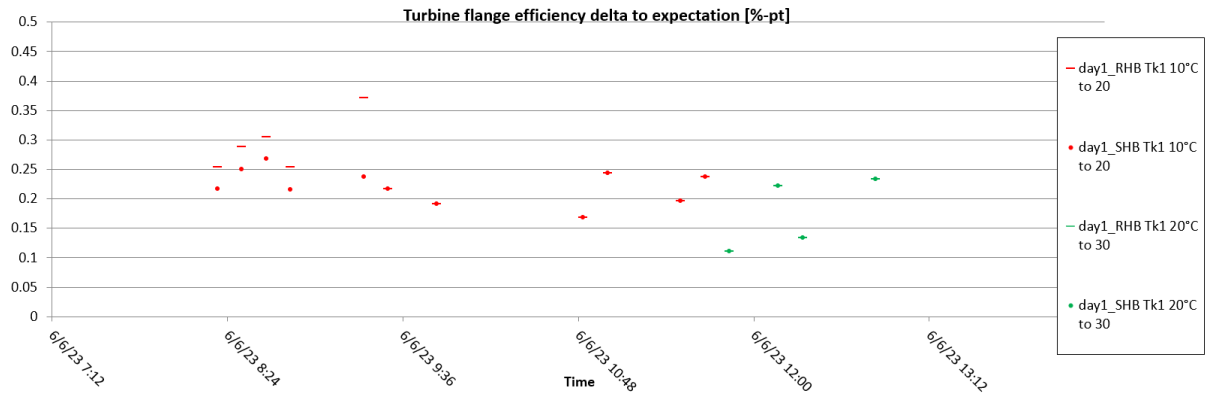


Figura 3.23 Turbine flange efficiency delta to expectation ansyn factor

From the previous figures, it is clear how incorrect measurements can affect the results of heat balances and thus the performance estimate. In fact, Figure 3.24 shows the temperature at the combustor outlet, and it can be seen how incorrect measurements affect the evaluation of it, which can lead to a variation of about 10 K. The hot gas temperature is considered confidential so it is not possible to show absolute values, therefore normalized results are shown.

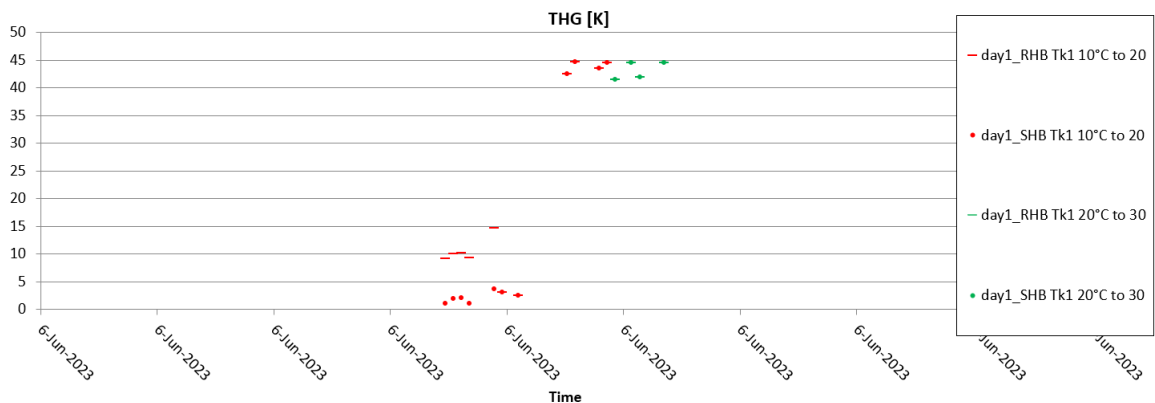


Figure 3.24 Wrong measurements effects on hot gas temperature

Problems in measuring the exhaust pressure of the GT turbine at another plant emerged in September 2023. As shown in Figure 3.25, fluctuations are observed in the measurement of the turbine exhaust pressure, suggesting a malfunction of the sensors.

Furthermore, the second pre-processing of the measurements also identified the flow measurement in the MBH30 pipe as incorrect and a measurement error in the inlet pressure loss. These errors therefore affect the performance calculations.

report first script

```

INFO MP 2023-09-27_19.39.00_19.40.00
Measurement Raw value Corrected value
MBL30CP013_XQ01 -0.5755615234375 1.1981139525367
MBA30CP001_XQ01 1.02268653315972 1.03316291772938
MBA30CP002_XQ01 1.02480047951076 1.03316291772938
MBA30CP003_XQ01 1.0208425668115 1.03316291772938

INFO MP 2023-09-27_19.49.00_19.50.00
Measurement Raw value Corrected value
MBL30CP013_XQ01 -0.5755615234375 1.2061426623207
MBA30CP001_XQ01 1.02210452975738 1.03062396521948
MBA30CP002_XQ01 1.02474305386246 1.03062396521948
MBA30CP003_XQ01 1.02117899928279 1.03062396521948

INFO MP 2023-09-27_19.59.00_20.00.00
Measurement Raw value Corrected value
MBL30CP013_XQ01 -0.5755615234375 1.2101432312158
MBA30CP001_XQ01 1.02265378355889 1.02835803558775
MBA30CP003_XQ01 1.02163015554963 1.02835803558775

```

report second script

```

MP: 2023-09-27_19_39_00_19_40_00
RAW VALUE SMOOTHED VALUE
MBH30CF020_CALC 542760 999511

MP: 2023-09-27_19_49_00_19_50_00
RAW VALUE SMOOTHED VALUE
MBH30CF020_CALC 103161 994655

MP: 2023-09-27_19_59_00_20_00_00
RAW VALUE SMOOTHED VALUE
MBH30CF020_CALC 472320 143747

```

Figure 3.25 Pre-processing script report 27/09/2023

These incorrect measurements have a direct effect on the compressor's inlet flow rate, as can be seen from Figure 3.26. Consequently, as the fuel flow rate is fixed, this affects the hot gas temperature. In figure 3.27 a normalized hot gas temperature is shown, in this case the RHB hot gas temperature is approximately 10 K higher.

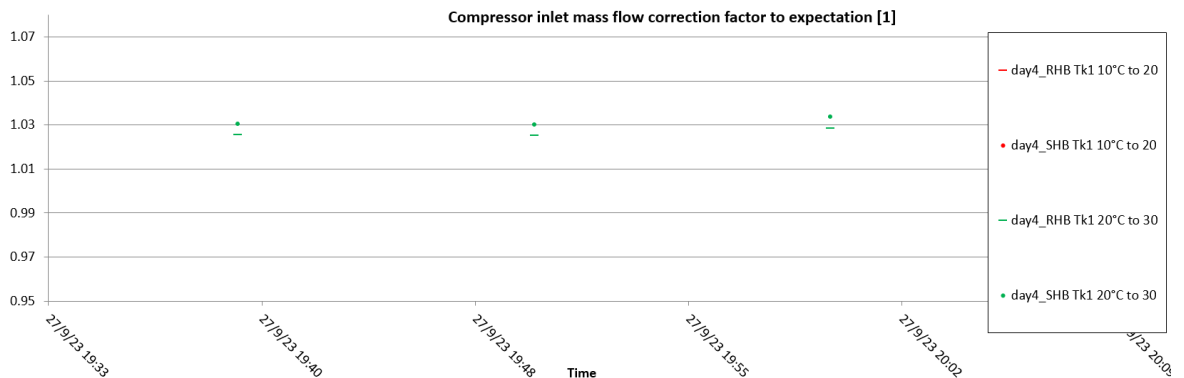


Figure 3.26 Compressor inlet massflow ansyn factor

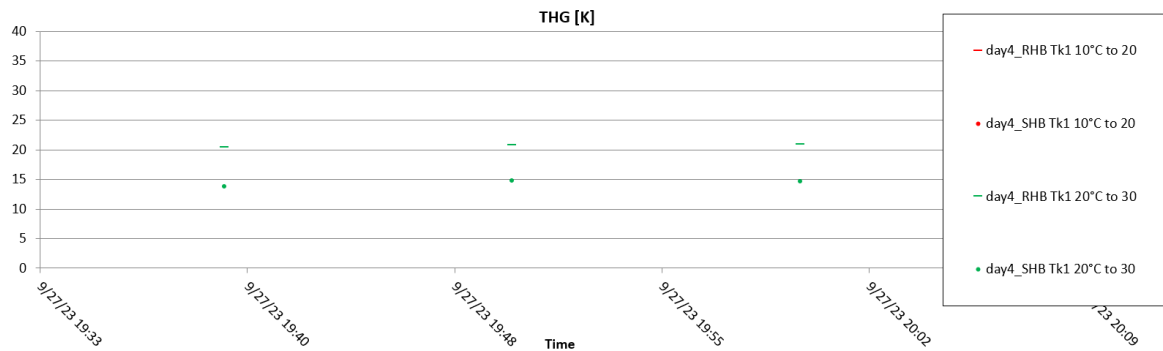


Figure 3.27 Wrong measurements effects on hot gas temperature

From the above results, it is possible to deduce the sensitivity of the software due to measurement errors. An in-depth analysis makes it possible to understand what the concomitant effects are of having incorrect measurements on each of the efficiency parameters of the components.

To show the sensitivity of transients instead, an example of MP sampled immediately after a load ramp is shown in Figure 3.28, in order to highlight the reason for the need for a stabilisation criterion. To demonstrate this, an ansyn factor particularly sensitive to such transients is used, which is defined on the efficiency of the first compressor sector. This sector is between the inlet and the first extraction point of the cooling flow (MBH10). The ansyn is defined as the delta to expectation and shows, in figure 3.29, how the heat balances tend to diverge from the average trend as they are at the section following the load ramp.

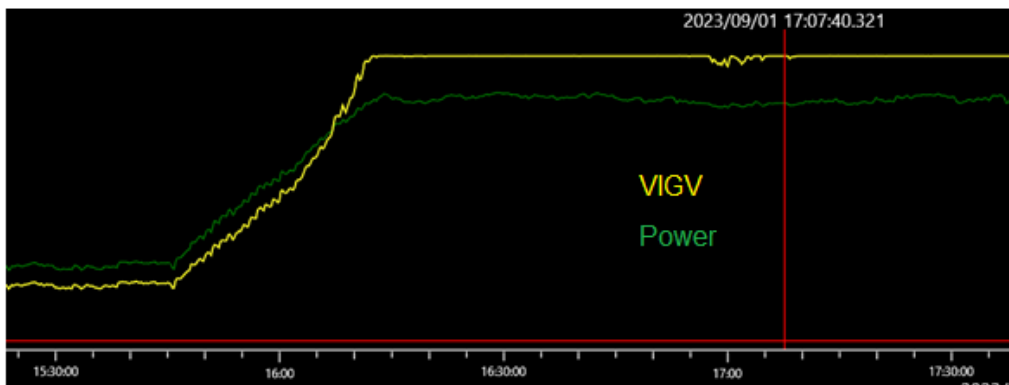


Figure 3.28 OvData viewer shows load ramp in commercial operation

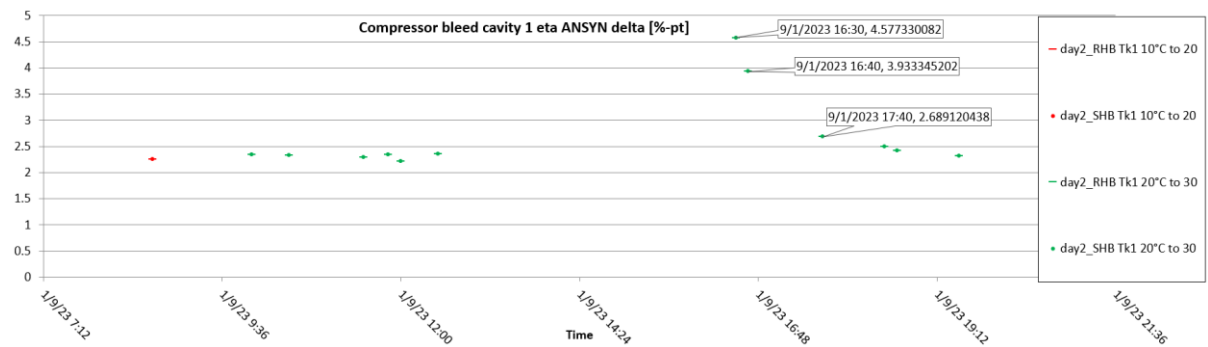


Figure 3.29 First sector compressor efficiency

Finally, an example is given of heat balances carried out in February in Marghera on two different days. The second day analysed was specifically chosen following the compressor wash, and in figure 3.30 it is possible to see how there is an increase in efficiency. Indeed, remember that the ansyn factor is defined as the difference between the efficiency of the heat balance and the efficiency predicted by the model. Consequently, the calculated efficiency tends to increase as the compressor is washed. Figure 3.31 also shows the ansyn factor on

the compressor's reduced flow rate, which clearly shows an increase as a result of flushing. In the latter, a deviation between RHB and SHB can be seen due to the correction of the total flow rate of the MBH30 system.

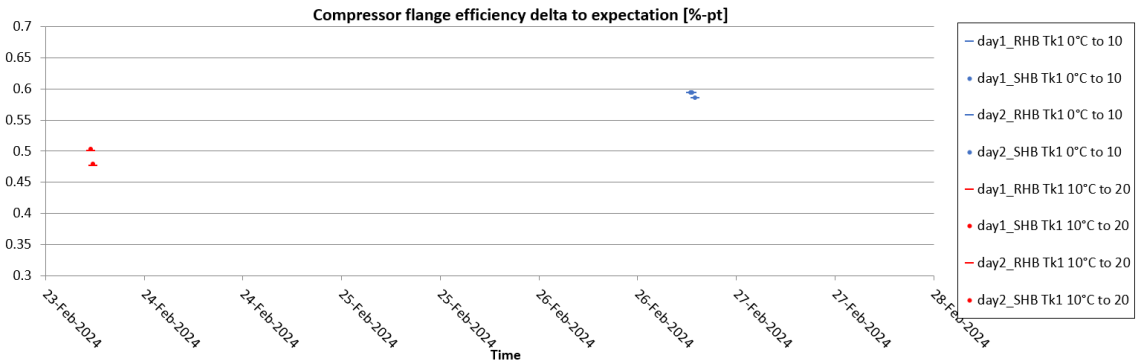


Figure 3.30 Compressor washing effect on compressor efficiency ansyn factor

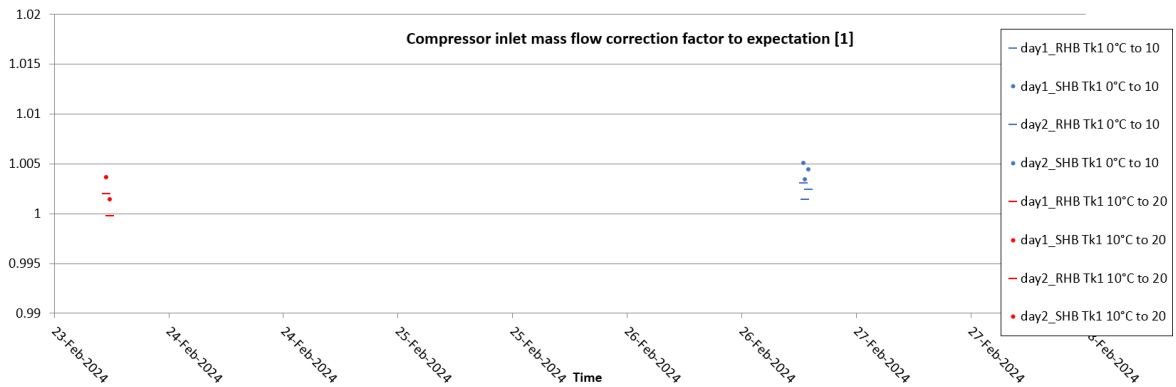


Figure 3.31 Compressor washing effect on inlet massflow ansyn factor

4. Conclusions

In conclusion, we reviewed the results obtained from the measurement pre-processing system, highlighting the importance of having a pre-processing system to enable more frequent monitoring than previous practices. The effectiveness of the measurement processing system successfully identified the problems encountered in the field, detecting wrong measurement and faulty sensors, confirming the accuracy of the pre-processing system.

The importance of having a monitoring system to continuously monitor gas turbine (GT) performance was also highlighted, highlighting the sensitivity of the performance tool to different degradation conditions and thermal transients. This underlines the potential of the system in detecting serious component problems, allowing the manufacturer to take preventive action to avoid outage.

This system also allows a distinction to be made between the true degradation of the GT and the degradation of the measuring instruments, enabling dual monitoring of both the actual state of the engine and the state of the fitted sensors. This allows the performance team to develop a deeper understanding over time of which measurements to rely on to develop heat balances and evaluate component performance, finding alternatives in the event of persistent measurement problems.

Over time, it will be important to develop the necessary sensitivity to define the tolerances within which measurements can deviate from the value predicted by the model, making it possible to verify the normal degradation of the GT without excessive intervention and thus without losing useful information.

The analysis of the results also revealed the importance of having an accurate model of the gas turbine, calibrated as best as possible, so that reliable reference values can be used to correctly estimate GT performance even in the event of proven faulty measurements.

The project discussed in this thesis has as its future perspective the implementation of an increasingly advanced automation of the monitoring process, which will allow performance results to be obtained in real time. This future goal, called 'Online Automated Heat Balance', will be crucial for Ansaldo Energia, as it will not only allow constant monitoring of performance, but also early warnings in the event of serious damage to the gas turbine. The implementation of this automated monitoring system will represent a significant step forward in the industry, enabling proactive management of gas turbine performance. Early warnings will allow technical personnel to act promptly to prevent further damage and ensure optimal plant operation. This future perspective highlights the importance of continuing to develop and improve monitoring technologies in the energy sector to ensure more efficient, safe and reliable production.

REFERENCES

- [1] Ansaldo energia website. <https://www.ansaldoenergia.com>, 2023
- [2] Meherwan P. Boyce. *Gas Turbine Engineering Handbook*. Gulf Professional Publishing, 2002.
- [3] G. Lozza. *Turbine a gas e cicli combinati*. Esculapio edizioni, Italia, 2016.
- [4] H. Taniguchi, Sigehiro Miyamae, *Power Generation Analysis for High-Temperature Gas Turbine in Thermodynamic Process*, 2000.
- [5] A. Massardo, *Analisi del funzionamento in condizioni fuori progetto degli impianti turbogas e cicli combinati*, corso di Impianti per l'energia, 2020.
- [6] M. Ubaldi, *Combustori di turbine a gas*, corso di Combustione, 2022.
- [7] P.P. Walsh, P. Fletcher, *Gas Turbine performance*, Second Edition
- [8] International Standard, ISO 2314 Gas Turbine – Acceptance tests, Third Edition 2009.

Nomenclature

Symbols

W	[W]	Power
P	[W]	Power
\dot{m}	[kg/s]	mass flow rate
T	[K]	Temperature
P	[bar]	Pressure
ρ	[kg/m ³]	Density
LHV	[J/kg]	Fuel low heat value
R	[J kg ⁻¹ K ⁻¹]	Gas constant
c_p	[J kg ⁻¹ K ⁻¹]	Isobaric specific heat capacity
c_v	[J kg ⁻¹ K ⁻¹]	Specific heat capacity at constant volume
n	[rpm]	Rotational speed
s	[J kg ⁻¹ K ⁻¹]	Specific entropy
h	[J kg ⁻¹]	Specific enthalpy
η	[-]	Efficiency
γ	[-]	Gas specific heat ratio
π	[-]	Pressure ratio
α	[°]	Flow angle
ζ	[-]	Pressure loss coefficient
λ	[-]	Diffuser recovery factor
ε	[-]	Pressure loss coefficient

Superscripts and Subscripts

*	Total stagnation property
c	Compressor

CO	Compressor
t	Turbine
TU	Turbine
a	air
f	fuel
n	net
in	inlet
ideal	ideal
cycle	cycle
corr	corrected
ref	reference
hg	hot gas
SOT	stator outlet temperature
ISO	Refers to ISO condition
loss	losses
shaft	Shaft
mech	Mechanical
geno	Generator
s	sensible
E,i	Compressor Extration, number i
bl	Blading
rel	Relative
p	Polytropic
CC	Combustion chamber

dif	Diffuser
supply	referes to supply conditions
sink	Refers to sink conditions
HB	Refers to heat balance
SYN	Refers to synthesis calculation

Abbreviations

TIT	Turbine inlet temperature
TAT	Temperature after turbine
ANSYN	Analysis by synthesis
HB	Heat balance
BOP	Block oriented process
MP	Measurement point
GT	Gas turbine
MDP	Measurement data preparation
RHB	Raw heat balance
SHB	Smoothed heat balance
CA	Cooling air
CAC	Cooling air cooler
VIGV	Variable guide vane
SAS	Secondary air system
TCLA	Turbine cooling and Leakage air
FB	First burner
SB	Sequential burner

